catalysts

MDPI

Review

The Biochemistry of Artificial CO_2-Fixation Pathways: The Exploitation of Carboxylase Enzymes Alternative to Rubisco

Immacolata C. Tommasi

Dipartimento di Chimica, Università di Bari Aldo Moro, 70126 Bari, Italy; immacolata.tommasi@uniba.it

Abstract: The last decade has registered a rapid development of new artificial CO_2-bioconversion processes mirroring natural CO_2-fixation by carboxylation and/or reduction reactions. The development of artificial pathways has shown that we have sufficient tools to design and implement, both in vitro and in vivo, complex reaction sequences pointing to construct microbial cell-factories to produce target chemicals at scale. This review is aimed to focus on the most efficient artificial CO_2-fixing autotrophic cycles based on the use of carboxylase enzymes that, similarly to Rubisco enzyme, build a C–CO_2 bond by reacting an enediolate or an enolate anion with CO_2. The development of artificial CO_2-fixing autotrophic cycles encompasses the analysis of the complete library of natural carboxylase enzymes taking part in the so called "central" and "assimilation" metabolism to select only those enzymes characterized by high catalytic efficiency, great stability, high substrate affinity, and oxygen tolerability. The review analyzes the biochemistry of the most efficient artificial CO_2-fixation pathways implemented up today, evidencing the biosynthetic strategies adopted, the development of replenishing routes, and their integration with cell metabolism.

Keywords: artificial CO_2-fixation; carboxylases enzymes; cell-factories

Citation: Tommasi, I.C. The Biochemistry of Artificial CO_2-Fixation Pathways: The Exploitation of Carboxylase Enzymes Alternative to Rubisco. *Catalysts* **2024**, *14*, 679. https://doi.org/10.3390/catal14100679

Academic Editor: Francisco Valero

Received: 19 August 2024
Revised: 19 September 2024
Accepted: 24 September 2024
Published: 1 October 2024

1. Introduction

In Nature, carbon fixation is accomplished by autotrophic organisms, including plants, algae, and some bacteria. According to recent estimations, the global multi-year mean of gross primary production (GPP) over the 2001–2018 period ranges between 435.6–618.1 Gt of CO_2 per year [1,2], and about 95–98% of all CO_2 fixed is employed by carboxylase enzymes promoting C–CO_2 bond formation [3,4], while the remaining 5–2% is involved in biological reduction reactions with CO_2 conversion into HCOOH, CO, CH_3OH, or CH_4.

Since autotrophic organisms represent the first trophic level of food chain, it can be concluded that "autotrophic carboxylases" start fixing almost all carbon that feeds life on earth [3,4], with significant impact on annual CO_2 fluxes of the biosphere.

In an attempt to mimic Nature, great efforts have been made recently to implement, at industrial scale, biotechnological processes targeting fuels or chemicals production using CO_2 as a feedstock. Actually, using CO_2 as source of carbon is the main goal of the third generation biorefinery (3G biorefinery) that lies on utilization of cell factories growing directly on CO_2 and exploiting H_2 or renewable energy for the production of target chemicals [5]. In contrast, 1st (1G) and 2nd (2G) biorefinery generations were based on sugars and biomass, respectively, as feedstocks. As an example of a 3G biorefinery, it can be cited the OAKBIO Process using engineered bacteria fixing CO_2 through the Calvin–Benson–Bassham (CBB) cycle with subsequent reduction of intermediates to butanol [6,7].

CO_2-based biotechnologies on-stream today are expected to fulfill "sustainable" and "eco-friendly" claims, while their real economic feasibility and "climate benefit" are questioned and will be better estimated in the near future [8].

The development of biotechnology industry is supported by straightforward innovations, including progresses in the area of metabolic engineering, the incorporation of heterologous pathways into micro-organisms, and advanced recombination technologies [9].

Among top biotechnology innovations, a straightforward approach consists in assembling, in vitro, in cell-free conditions, selected enzymes extracted from various microorganisms featured to catalyze cascade reactions to operate "new-to-Nature" synthetic pathways. Whenever possible, efficient artificial pathways are implemented in vivo. Several interesting Reviews have focused recently on advances of metabolic engineering aiming at artificial CO_2 utilization [10–18], including reviews from the Erb Research Group [19], providing details about general principles for pathways design and implementation.

Most of the newly implemented artificial pathways fix CO_2 (or HCO_3^-) directly into "carrier molecules" that are regenerated at the end of the cycle, in strict analogy to most part of natural autotrophic pathways as the Calvin-Benson-Bassham cycle (CBB), the reductive citric acid cycle, the 3-hydroxypropionate-4-hydroxybutyrate cycle, the dicarboxylate-4-hydroxybutyrate cycles, and 3-hydroxyproionate bicycle [20]. Always in analogy to natural pathways, the artificial cycles synthesize metabolic intermediates entirely from CO_2.

As alternative to CO_2-fixation by carboxylase enzymes, other designed artificial pathways are fed by C1 species as CO, CH_3OH, HCOOH, or HCOH, which can be produced by CO_2 reduction reactions, both biochemically and electrochemically [21–23]. These pathways have usually (but not exclusively) a "linear" arrangement, meaning they do not regenerate the molecular carrier [24–26].

The present manuscript is meant to focus on the biochemistry of the recently published artificial CO_2-fixation pathways constructed around key carboxylase enzymes alternative to Rubisco, encompassing C–CO_2 bond formation through reaction with an enolate anion or an enediolate. Most of these newly designed artificial pathways have demonstrated practical feasibility, being implemented in vitro and/or in vivo. The review evidences the synthetic advantages brought by artificial cycles, allowing construction of new efficient metabolic wires after integration with natural pathways. Specific aspect concerning CO_2-fixation rate by the cycles, energy efficiency, and implementation of replenishing routes are also analyzed.

As the main goal of the present review is to focus on the synthesis of metabolic intermediates encompassing C–CO_2 bond formation, those pathways encompassing CO_2-reduction to other C1 species prior to assimilation into synthetic routes will not be dealt with here.

2. Cell-Free In Vitro Systems

As mentioned in the introductory section, the build-up of "cell-free", "new-to-Nature" synthetic pathways for CO_2 fixation into C2-intermediates (acetyl-CoA, glyoxylate, oxalate) has been recently implemented as powerful tools for metabolic engineering and synthetic biology. Cell-free systems are built assembling enzymes extracted from different organisms (including bacteria, plant, archaea, and humans) with subsequent system optimization through control of cofactors (NADPH, ATP, $FADH_2$) and metabolites concentrations.

The design of new synthetic enzymatic pathways requires at first in silico design of the artificial reaction sequence, followed by pathway optimization by machine learning algorithm. Careful pathways design ensures fast rate-limiting steps and favourable thermodynamics. Details concerning the design and implementation of "new-to-Nature" synthetic pathways can be found in recent literature [10,19]. The designed reaction sequence is finally tested in vitro and, (if possible) ultimately, in vivo.

One of the advantages of "cell-free" pathways construction over in vivo production by engineered microorganisms resides in the possibility to test the efficiency of hundreds to thousands of new different pathways in relatively short time, selecting the most efficient process and "mimicking" the selection operated by evolution. Moreover, enzymes from different living matter can be assembled in vitro, which never occur in Nature, including engineered enzymes [27].

As noted by Erb [28], testing in vitro efficient synthetic pathways opens up possible future applications including: (i) the possibility of transplanting in vivo the optimized pathways in lithotrophic or photosynthetic organisms; (ii) coupling the pathway in vitro

with artificial photosynthetic processes; (iii) building the base units for future artificial or minimal cells.

The following Section summarizes the biochemistry of recently published cell-free pathways. Some of those pathways, after being testing in vitro, have also been tested in vivo.

3. Computational Analysis of Artificial Carbon Fixation Pathways: The Malonyl-CoA-Oxaloacetate-Glyoxylate (MOG) Pathways

The computational design of artificial CO_2-fixation metabolic routes was started by Bar-Even et al. in 2010 [29,30].

The research group at first developed a computer-aided evaluation of several natural autotrophic carbon fixation pathways. The analysis brought to the conclusion that naturally occurring autotrophic synthetic pathways (including the Calvin–Benson–Bassham pathway) are already evolutionary optimized with respect to their environment. Thus, in an attempt to attain more efficient synthetic routes, a different approach must be adopted.

The work aimed to design autotrophic cycles as alternatives to the CBB cycle, constructed around carboxylase enzymes different from Rubisco. New pathways were designed assembling existing metabolic building blocks from various organisms and selecting enzymes from those reported in the Kyoto Encyclopaedia of Genes and Genomes (KEGG) database. The collection and comparison of the catalytic properties of various carboxylase enzymes evidenced more promising enzymes, as those with highest specific activity, affinity for the carbon source (CO_2 or HCO_3^-) and oxygen tolerance. Interestingly, better-performing carboxylase enzymes, summarized in Table 1, have been selected as central carboxylating enzymes in artificial cycles developed during the last decade.

Table 1. Catalytic properties of several carboxylase enzymes as evaluated by Bar-Even [29].

Enzyme Name (EC Number)	Carbon Species	Specific Activity [a] μmol min^{-1} mg^{-1} (at Saturating CO_2/HCO_3^-)	Km (mM) [a] for Carbon Substrate	Co-Factors
Rubisco (4.1.1.39)	CO_2	3.5	0.01–0.02	-
Crotonyl-CoA carboxylase/reductase (1.3.1.85)	CO_2	130	14	NADPH
Phosphoenolpyruvate carboxylase (4.1.1.31)	HCO_3^-	35	0.06–0.2	-
Phosphogluconate dehydrogenase (1.1.1.41-42)	CO_2	0.6	15–50	NADPH

[a] the values have been taken from reference [29]. The table shows the average of values collected from the literature.

Considering the specific activity of known carboxylase enzymes, phosphoenolpyruvate carboxylase (Pepc) emerged as a very attractive enzyme with a catalytic activity of 35 mmol of CO_2 fixed min^{-1} mg of $protein^{-1}$, superior affinity towards HCO_3^- (Km = 0.06–0.2 mM), and oxygen insensitivity. Consequently, new synthetic carbon fixation pathways, called "malonyl-CoA-oxaloacetate-glyoxylate" (MOG) pathways, were designed that employ phosphoenolpyruvate carboxylase (Pepc) as a central enzyme, along with additional enzymes from the natural C4-plant cycle. Interestingly, the designed metabolic routes have a cyclic arrangement, i.e., CO_2 is integrated into carrier molecules undergoing chemical transformation and ultimately regenerated at the end of the cycle in order to start a new round.

Scheme 1 shows one of the designed MOG cycles named C4-glyoxylate cycle (including alanine as co-substrate).

As shown in Scheme 1, the reactions starting the MOG pathway convert pyruvate into malate in a reaction sequence similar to the cycle adopted by C4-plants to concentrate CO_2 into bundle cells. It can be noted that formally 2 mol of pyruvate enters the cycle, being converted into 2 mol of oxaloacetate (evidenced by black and blue arrows in Scheme 1). Subsequently, the 2 mol of oxaloacetate have different fates: 1 mol of oxaloacetate is

converted into malate, which is then activated into malyl-CoA intermediate and split into glyoxylate and acetyl-CoA. The remaining 2nd mol of oxaloacetate transfers the carboxy-group to acetyl-CoA, regenerating pyruvate (which is recycled in reaction 1) and producing malonyl-CoA by the key enzyme methylmalonyl-CoA carboxytransferase (reaction 6). Malonyl-CoA is subsequently reduced to malonate semialdehyde, which undergoes a transamination reaction with co-substrate α-alanine, affording β-alanine and pyruvate (once again recycled in reaction 1). Finally, β-alanine 2,3-aminomutase converts β-alanine into α-alanine, re-entering the cycle.

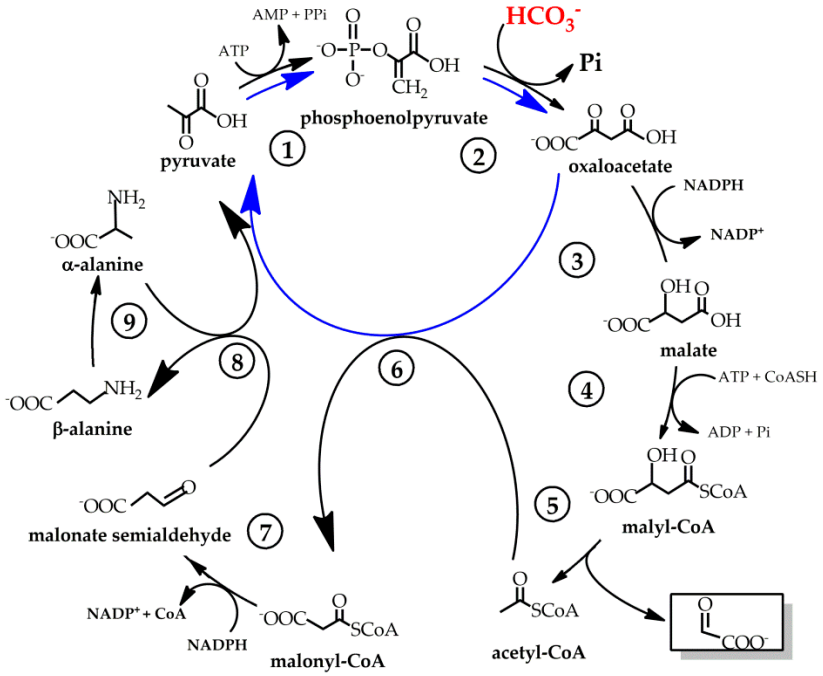

Scheme 1. The malonyl-CoA-oxaloacetate-glyoxylate (MOG) pathway, named C4-glyoxylate cycle (including alanine as co-substrate). Formally, it can be considered that reactions 1 and 2 proceed converting 2 mol of pyruvate into 2 mol of oxaloacetate (black arrow + blue arrow). The 2 mol of axaloacetate produced undergo a different pathway conversion: 1 mol of axaloacetate is converted into malate, malyl-CoA and, finally, into acetyl-CoA. The other is engaged in acetyl-CoA transcarboxylation, regenerating pyruvate. Reaction 1: pyruvate water/phosphate dikinase; reaction 2: phosphoenolpyruvate carboxylase; reaction 3: malate dehydrogenase; reaction 4: malyl-CoA synthetase; reaction 5: malyl-CoA lyase; reaction 6: methylmalonyl-CoA carboxytransferase; reaction 7: malonate-semialdehyde deidrogenase; reaction 8: β-alanine-pyruvate transaminase; reaction 9: alanine 2,3-aminomutase. Absolute or relative configurations of chiral centers are reported only if specified in the original source. (Scheme from ref. [29], adapted and used from original source distributed under the PNAS open access option).

It can be noted that the overall stoichiometry of the cycle is:

$$2\ HCO_3^- + 2\ ATP + 2\ (NADPH + H^+) \rightarrow glyoxylate + ADP + Pi + AMP + PPi + 2\ NADP^+ \quad (1)$$

Glyoxylate is a metabolic intermediate that, in vivo, could potentially enter the bacterial-like glycerate pathway, ultimately being converted into glyceraldehyde-3-phosphate (GA3P). Therefore, in photosynthetic organisms, CO_2-fixed into glyoxylate may enter the CBB cycle.

Since the pioneering work of Bar-Even's Group approximately 30 artificial pathways have been designed and theoretically evaluated up today. Most of the designed theoretical cycles that have found implementation in vitro and/or in vivo are described in the following Sections.

4. Artificial Synthetic Pathways Fixing CO_2 through C-CO_2 Bond Formation

Most part of Natural accredited autotrophic CO_2-fixation pathways (Calvin–Benson–Bassham, reductive citric acid, 3-hydroxypropionate-4-hydroxybutyrate, dicarboxylate-4-hydroxybutyrate cycles, and 3-hydroxyproionate bicycle) are cyclic pathways. In these, a primary CO_2-acceptor molecule undergoes chemical transformation and regeneration at the end of the sequence, allowing a second cycle to start. The cycle may undergo subsequent rounds as long as additional reagents (including NAD(P)H and ATP coenzymes) are available and kinetic and thermodynamic requirements are satisfied.

Most part of designed synthetic pathways have mimicked the cyclic arrangement of the natural autotrophic cycles. Examples of these "new-to-Nature" pathways are described in the remainder of this section to give an overview of the chemistry exploited and strategies adopted to solve problems as cofactor requirements, metabolite concentration optimization, and natural anapleurosis mimicking.

4.1. Artificial Pathways Based on Enoyl-CoA Carboxylase Enzymes: The CETCH Cycle

The first "new-to-Nature" cycle designed and subsequently performed in vitro was reported by Erb et al. in 2016 [31]. The acronym CETCH includes names from three key enzymes of the cycle: crotonyl-CoA carboxylase/reductase, ethylmalonyl-CoA mutase, and hydroxybutyryl-CoA dehydratase.

The CETCH cycle (shown in Scheme 2) has been set after theoretical design of six diverse alternative cycles, all based on the use of crotonyl-CoA carboxylase/reductase enzyme.

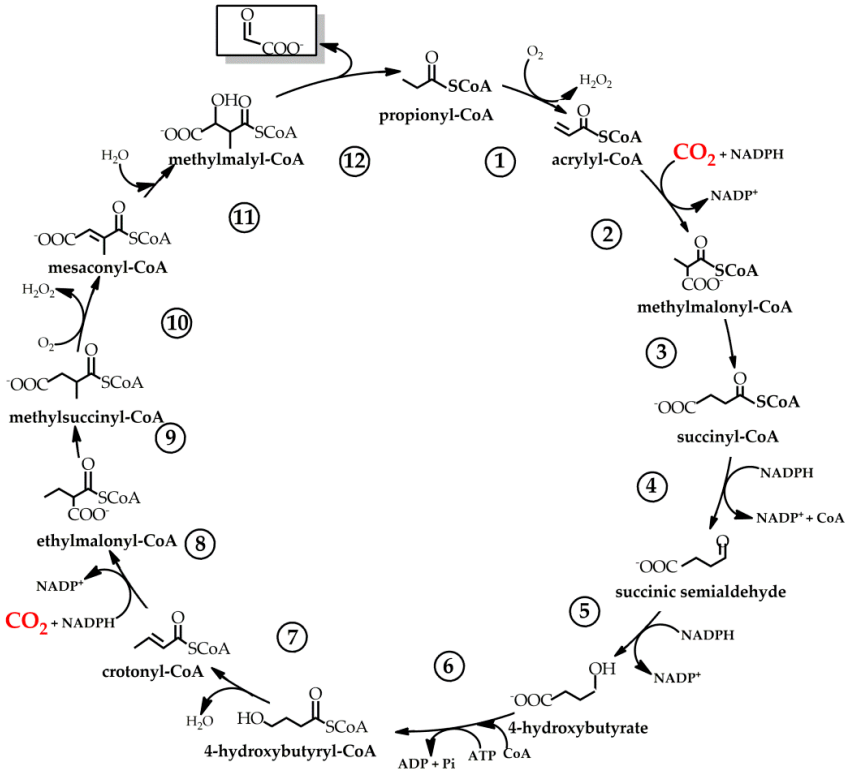

Scheme 2. The CETCH cycle (version 5.4) performed in vitro. Reaction 1: propionyl-CoA oxidase; reaction 2: crotonyl-CoA carboxylase reductase; reaction 3: methylmalonyl-CoA mutase and emC/mmCepimerase; reaction 4: succinyl-CoA reductase; reaction 5: succinic semialdehyde reductase; reaction 6: 4-hydroxybutyryl-CoA synthetase; reaction 7: 4-hydroxybutyryl-CoA dehydratase; reaction 8: crotonyl-CoA carboxylase reductase; reaction 9: ethylmalonyl-CoA mutase and emC/mmCepimerase; reaction 10: methylsuccinyl-CoA oxidase; reaction 11: mesaconyl-CoA hydratase; reaction 12: β-methylmalyl-CoA lyase. Absolute or relative configurations of chiral centers are reported only if specified in the original source. (Scheme from reference [31], adapted and used by permission of AAAS (copyright© 2016).

Crotonyl-CoA carboxylase/reductase enzymes (Ccr) belong to enoyl-CoA carboxylases (ECR) class, recently discovered in *α-proteobacteria* and *Streptomicetes* families [32]. As far as is known, ECRs are not present in the accredited natural autotrophic CO_2-fixation pathways, as they are mainly involved in assimilation metabolism. However, ECR enzymes shares several useful molecular peculiarities as: (i) a broad substrate spectrum; (ii) oxygen insensitivity; (iii) NADPH requirement (only) as cofactor; and (iv) a catalytic efficiency of $7.1 \pm 5.1\ 10^5\ M^{-1}\ s^{-1}$, which approximately doubles the value of $2.9 \pm 1.1\ 10^5\ M^{-1}\ s^{-1}$ measured for Rubisco.

Experimentally, the final version of the cycle (5.4 version, shown in Scheme 2) was set after repeated feasibility tests, that is, after reconstituting the central reaction sequence stepwise, testing (and correcting) for undesired interactions of enzymes and cofactors.

Propionyl-CoA substrate, acting as the acceptor molecule, is dehydrogenated to acrylyl-CoA and subsequently carboxylated to methylmalonyl-CoA (reaction 2) from a crotonyl-CoA carboxylase/reductase enzyme (from *Methylorubrum extorquens*), which requires the NADPH cofactor. Five subsequent reactions convert methylmalonyl-CoA into crotonyl-CoA, which is further carboxylated to ethylmalonyl-CoA (by the same crotonyl-CoA carboxylase/reductase enzyme). Therefore, the same enzyme catalyzes both 2 and 8 reactions.

It is worth noting that, according to the Authors, NADPH transfers the hydride to the C3-carbon of acrylyl-CoA or (*E*)-crotonyl-CoA, while carboxylation occurs at C2-carbon to form (2*S*)-methylmalonyl-CoA or (2*S*)-ethylmalonyl-CoA, respectively [33], suggesting CO_2-interaction with an enolate anion (Scheme 3).

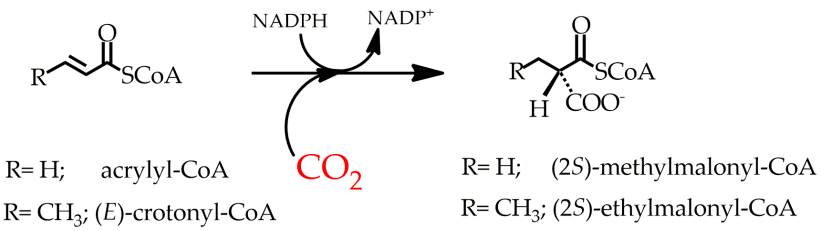

Scheme 3. Stereochemistry of reductive carboxylation of acryl-CoA and crotonyl-CoA by crotonyl-CoA carboxylase/reductase (Ccr) enzyme.

Subsequently, reaction 9 of the CETCH cycle is catalyzed by ethylmalonyl-CoA mutase, which isomerizes ethylmalonyl-CoA into methylsuccinyl-CoA, building the ramified C5-skeleton suitable for conversion into methylmalyl-CoA (reactions 10 and 11). The latter is split into glyoxylate and propionyl-CoA by the β-methylmalyl-CoA lyase (reaction 12) from *Rhodobacter sphaeroides*.

Overall, twelve consecutive reactions are catalyzed by eleven core enzymes, collected from bacteria, archaea, plants, and humans that were expressed in *E. coli*, purified, and fully characterized before being tested in vitro. Addition of several auxiliary enzyme was necessary to enable multiple turnover of the cycle (see Equations (3)–(5)).

In this respect, the Authors note that CETCH pathway exploit a marked advantage over natural evolution: "it gathers efficient enzymes from different domain of life that could never be collected naturally in one system". Moreover, in several key steps, not only "known reactions" were selected, but catalysis of "new" reactions with the required specificity and kinetics was achieved via protein engineering. For example, methylsuccinyl-CoA dehydrogenase required engineering techniques to be transformed into a methylsuccinyl-CoA oxidase (reaction 10), with concomitant O_2 reduction to H_2O_2. Methylsuccinyl-CoA oxidase was used in the final version of the cycle.

Experimentally, the overall cycle is started by addition of propionyl-CoA in a buffer containing $NaHCO_3$ and catalyzes the net conversion of 2 CO_2 into glyoxylate according to Equation (2).

$$2\ CO_2 + ATP + 4\ (NADPH + H^+) + 2\ O_2 \rightarrow \text{glyoxylate} + ADP + Pi + 4\ NADP^+ + 2\ H_2O_2 \quad (2)$$

CO_2 is fixed at a specific fixation rate of 5 nmol min^{-1} mg^{-1} of proteins (considering only proteins strictly involved into the cycle), which compares with the rate of 1–3 nmol min^{-1} mg^{-1} of proteins measured in cell extracts catalyzing the CBB cycle.

Most importantly, the CETCH cycle uses around 30% less ATP compared to CBB cycle. The efficiency of the CETCH cycle is largely due to use of the recently discovered enoyl-CoA reductase/carboxylase, the most active carboxylase enzyme known up today, and the implementation of an NADPH and ATP regeneration system to satisfy biochemical and thermodynamic requirements.

In fact, NADPH and ATP, supplied at the start, are regenerated during cycle's functioning thanks to the addition of formate dehydrogenase and polyphosphate kinase enzymes, and their relevant substrates (formate and polyphosphate, respectively). In particular, NAD(P)H regenerates according to the reverse of Equation (3), while ATP regenerates according to Equation (4).

$$CO_2 + NAD(P)H + H^+ \rightarrow HCOOH + NAD(P)^+ \quad (3)$$

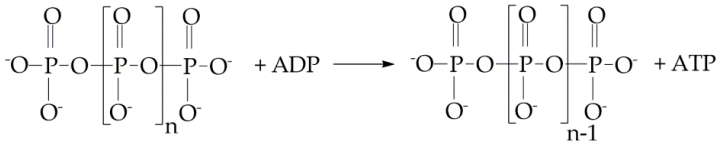

(4)

Interestingly, an engineered formate dehydrogenase was supplied that accept both NAD^+ and $NADP^+$ as substrates.

Moreover, in reactions 1 and 10 of the cycle (Scheme 2), the dehydrogenation of propyonyl-CoA and methylsuccinyl-CoA is accomplished with concomitant O_2 reduction to H_2O_2. The toxic effect of peroxide over proteins is prevented by the addition of catalase enzyme (Equation (5)).

$$2\ H_2O_2 \rightarrow 2\ H_2O + O_2 \quad (5)$$

Considering that NADPH regeneration with formate supply liberates CO_2 (Equation (3)), in a more recent work, Erb's Group faced the problem of energy supply requirement by coupling the CETCH cycle to the photosynthetic production of NAD(P)H and ATP by thylakoid membranes of *Spinacea oleracea* [34]. Thylakoid membranes from chloroplasts were isolated and encapsulated into water-oil microdroplets of around 92 µm in diameter (Figure 1).

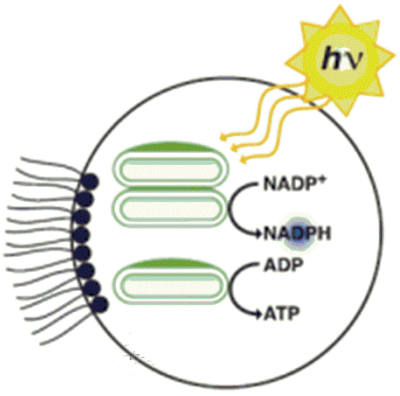

Figure 1. Graphic representation of water-oil microdroplets containing TEM (Thylakoid Energy Module) based on membranes of *Spinacea oleracea* producing NADPH and ATP by photosynthesis. (Figure from reference [34], adapted and used by permission of AAAS (copyright© 2020)).

Before encapsulation into water-oil microdroplets, thylakoid membranes were tested for their light-dependent activity in $NADP^+$ reduction to NADPH and ADP phosphorylation to ATP.

In particular, under irradiation at 100 µmol photons m^{-2} s^{-1}, the membranes catalyzed reduction of $NADP^+$ to NADPH (with concomitant O_2 evolution) at a specific activity of 3.41 ± 0.01 µmol min^{-1} mg^{-1} of total chlorophyll. $NADP^+$ reduction was dependent on external ferredoxin addition (5 µM), and prolonged membrane activity was obtained by addition of ROS (reactive oxygen species) scavengers (as superoxide dismutase and catalase enzymes).

Under optimized condition (irradiation at 60–70 µmol photons m^{-2} s^{-1}), thylakoid membranes catalyzed phosphorylation of ADP to ATP at a specific activity of 6.5 ± 0.5 mM min^{-1} mg^{-1} of total chlorophyll. Thanks to NADPH and ATP regeneration ability, the membranes were named Thylakoid Energy Module (TEM).

The TEM-containing microdroplets (containing approximately 100 TEM granules per droplet) were subsequently charged with the core enzymes of the CETCH cycle (upgraded to a 7.0 version to resolve interference of several metabolites), providing light-dependent production of NADPH and ATP.

The complete droplet system was irradiated at 50 µmol photons m^{-2} s^{-1} to produce glyoxylate with a carbon fixation rate of 0.21 µmol of CO_2 fixed mg^{-1} of chlorophyll h^{-1}. The Authors commented that the rate of CO_2-fixation by the complex system was lower if compared with the carbon fixation rate when crotonyl-CoA carboxylase/reductase alone was encapsuled into droplets (6.4 µmol of CO_2 fixed mg^{-1} of chlorophyll h^{-1}). However, the experiment provides evidence that an artificial system may successfully integrate an artificial CO_2-fixation pathways with light-promoted NADPH and ATP production.

4.2. Integration of the CETCH Cycle with Other Pathways and Anapleurosis

In view of integrating the CETCH cycle into living organisms, acetyl-CoA is a desirable universal metabolic intermediate suitable for connecting an artificial synthetic pathway to natural biosynthetic routes for the ultimate synthesis of sugars, fatty acids, and proteins. To this end, glyoxylate produced by CETCH cycle must be converted into acetyl-CoA. Erb et al. have coupled the CETCH cycle to the natural β-hydroxyaspartate cycle (BHAC) used by marine proteobacteria for glyoxylate assimilation, enabling conversion of glyoxylate into oxaloacetate (Scheme 4) [35].

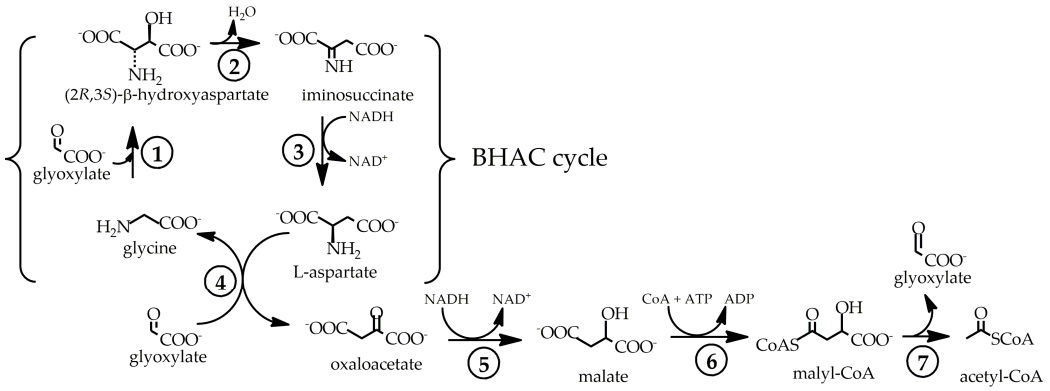

Scheme 4. The β-hydroxyaspartate (BHAC) cycle (reactions 1–4) integrated with (part of) serine cycle (reactions 5–7) for glyoxylate conversion into acetyl-CoA. Reaction 1: β-hydroxyaspartate aldolase; reaction 2: β-hydroxyaspartate deidratase; reaction 3: iminosuccinate reductase; reaction 4: aspartare-glyoxylate aminotransferase; reaction 5: malate deidrogenase; reaction 6: malate thiokinase; reaction 7: malyl-CoA lyase. Absolute or relative configurations of chiral centers are reported only if specified in the original source. (Scheme from ref. [35], adapted and used from original source distributed under the Creative Common-Attribution Licence).

As shown in Scheme 4, the BHAC cycle is started by reaction 1, which converts glycine and glyoxylate into (2*R*,3*S*)-β-hydroxyaspartate by the β-hydroxyaspartate aldolase enzyme. Subsequent (2*R*,3*S*)-β-hydroxyaspartate dehydration (reaction 2) and reduction (reaction 3) produce L-aspartate, which undergoes transamination with a second glyoxylate

molecule to lead glycine (which is recycled into BHAC cycle) and oxaloaceate. Therefore, the net reaction of the cycle allows glyoxylate conversion into oxaloacetate according to Equation (6).

$$2\ \text{glyoxylate} + \text{NADH} + \text{H}^+ \rightarrow \text{oxaloacetate} + \text{NAD}^+ + \text{H2O} \quad (6)$$

To convert oxaloacetate into acetyl-CoA, the BHAC cycle was integrated with three additional reactions of the serine cycle (reactions 5–7 in Scheme 4).

Overall, running CETCH + BHAC + (part of) serine cycle in optimized experimental conditions (and adopting NADPH and ATP regeneration conditions) allows obtaining acetyl-CoA with a 30% yield (for net conversion of glyoxylate into acetyl-CoA) after 3 h of reaction.

The relatively low yield was due to reaction 7 (Scheme 4), which has a $\Delta G^\circ = -3 \pm 5.9$ kJ mol^{-1}, resulting in an equilibrium mixture of malyl-CoA, glyoxylate, and acetyl-CoA. To overcome this limitation, the reaction sequence shown in Scheme 4 was coupled to downstream reactions using acetyl-CoA to feed a biosynthetic route (nine enzymes of the mevalonate biosynthetic pathways and various terpene synthases shown in Scheme 5), producing mono- and sesqui-terpenes.

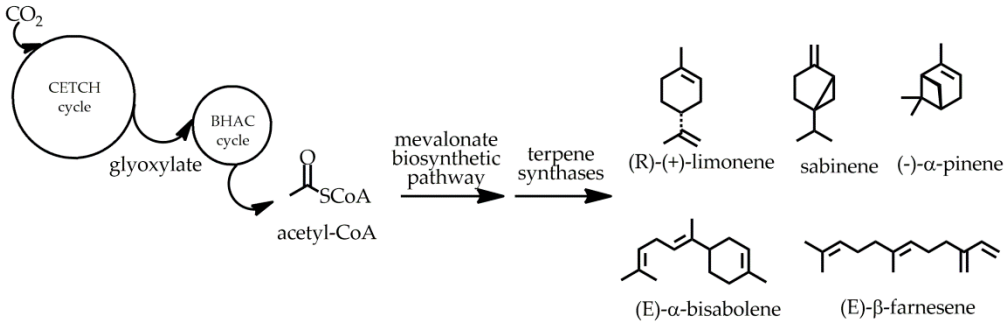

Scheme 5. Synthesis of mono- and sesqui-terpenes from acetyl-CoA produced by the artificial wire CETCH + BHAC + (part of) serine cycle + mevalonate biosynthetic pathway + terpene synthases. (Previously unpublished Scheme).

Under optimized experimental conditions (including cofactors re-generation reactions), mono- and sesqui-terpenes were obtained at concentration ranging from 20 to 40 μM over 24 h, reaching a productivity of 0.22 mg L^{-1} h^{-1}. The Authors note the obtained productivity is low if compared with productivity of *S. cerevisiae* or *E. coli* fed with glucose (2 to 100 mg L^{-1} h^{-1}). However, terpenes obtained through the wire CETCH-BHAC-(part of) serine cycle + mevalonate biosynthetic pathway and terpene synthases are entirely "built" from CO_2 instead of glucose.

Using even more complex enzymatic systems, acetyl-CoA was also converted into lactons or 1,3,5, 7,9,11,13-pentadecaheptaene, a precursor of pentadecane.

In a view of approaching, as far as possible, the functioning of natural biosynthetic processes, the Erb Group attempted to introduce "anaplerosis" into artificial pathways [36].

Anaplerosis is the self-replenishing capability of natural cycles, consisting in production of several intermediates by collateral pathways so that, with proper kinetics, optimal metabolite concentrations are constantly maintained, even when intermediates are diverted to feed other biosynthetic routes.

Anaplerosis is classically exemplified by replenishing the four-carbon units intermediates in the Tricarboxylic Acids Cycle (TAC). Introducing anaplerosis into artificial pathways would allow the synthesis of target molecules (more complex than two-carbon units) and fully exploit the synthetic potential of artificial cycles.

To this end, the Erb Group has designed four alternative "anaplerotic pathways" aimed at feeding-back intermediates of the CETCH cycle (Scheme 6). In particular: (i) Module C was designed to replenish propionyl-CoA from acetyl-CoA; (ii) Modules A and B were

designed to replenish succinyl-CoA from malate or acetyl-CoA, respectively; and (iii) Module D was designed to replenish crotonyl-CoA from acetyl-CoA.

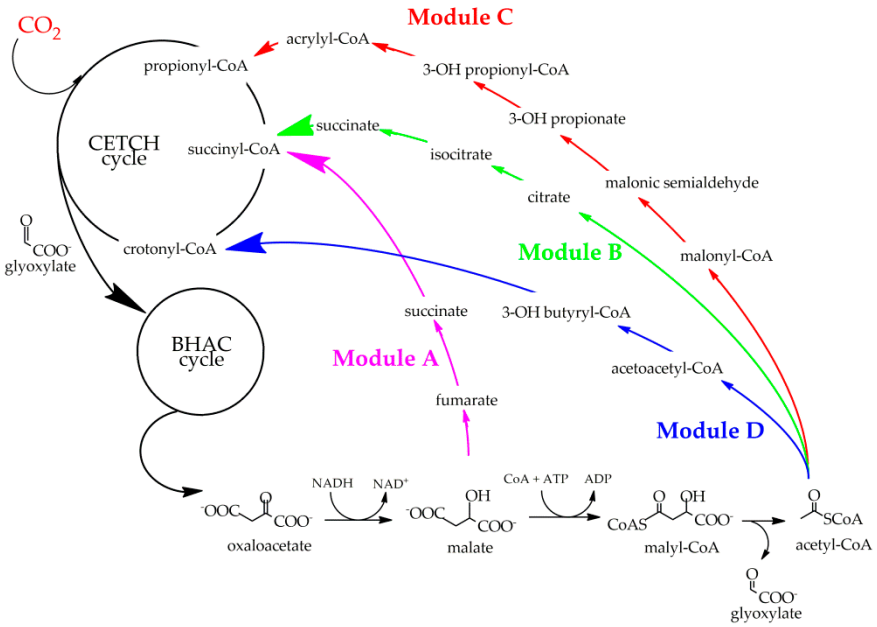

Scheme 6. Sequence of metabolites of the four designed CETCH replenishing Modules A–D and connection with the artificial wire CETCH + BHAC + (part of) serine cycle (oxaloacetate-malate-malyl-CoA-acetyl-CoA). Modules A (pink arrows) replenishes succinyl-CoA from malate; Module B (green arrows) replenishes succinyl-CoA from acetyl-CoA; Module C (red arrows) replenishes propionyl-CoA from acetyl-CoA; Module D (blue arrows) replenishes crotonyl-CoA from acetyl-CoA. Absolute or relative configurations of chiral centers are reported only if specified in the original source. (Previously unpublished Scheme).

Scheme 6 shows the sequence of metabolites of the four designed CETCH replenishing paths, converting malate or acetyl-CoA into CETCH intermediates. Each Module was designed with an optimized thermodynamic profile. Moreover, all used enzymes were selected to catalyze carbon conserving reactions and display oxygen insensitivity.

The artificial wire, composed of CETCH cycle + BHAC cycle + (part of) serine cycle + one replenishing module (one among modules A–D), was set up in an in vitro experiment gathering approximately 50 enzymes. To test the effectiveness of the overall synthetic wire in CO_2-fixation, the entire system was fed with glyoxylate (250 µM) and $NaHCO_3$, and the concentration of methylmalonyl-CoA (an intermediate of the CETCH cycle, Scheme 2) was monitored over time. Consequently, the carbon conversion yield was calculated. All the four replenishing modules demonstrated to be effective in methylmalonyl-CoA synthesis at concentration higher than 50 µM over 8 h. However, the highest methylmalonyl-CoA concentration was registered only with the use of the propionyl-CoA replenishing module C (shown in detail in Scheme 7). In fact, methylmalonyl-CoA concentration of around 500 µM of carbon after 8 h of monitoring was reached, allowing the calculation of a carbon conversion yield of 400%, proving significant CO_2-incorporation into the methylmalonyl-CoA metabolite.

It can be noted that the metabolite sequence of Module C (shown in Scheme 7) is the same as the 3-hydroxypropionate cycle [20]. However, the Authors avoided use of native enzymes of the 3-hydroxypropionate cycle, largely implementing engineered recently characterized enzymes. In particular: (i) reaction 1 in Scheme 7 is catalyzed by a propionyl-CoA carboxylase engineered to carboxylate acetyl-CoA to malonyl-CoA [37]; (ii) reaction 2 and 3 in Scheme 7 are catalyzed by a bifunctional malonyl-CoA/malonate semialdeide reductase [38]; (iii) reactions 4 and 5 in Scheme 7 are catalyzed by propionyl-CoA synthase,

a multicatalytic nanocompartment recently characterized [39]. Consequently, only three enzymes catalyze six reactions of Module C.

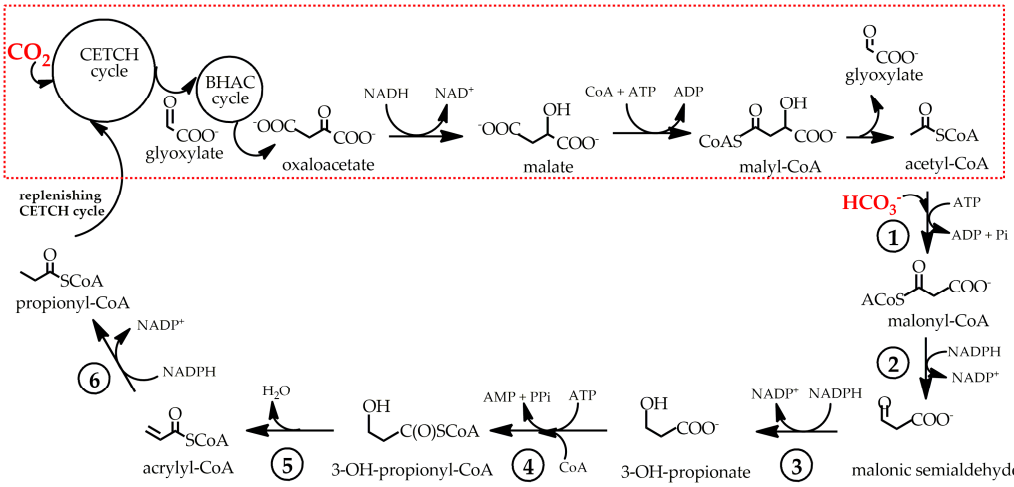

Scheme 7. Enzymatic reactions of Module C (reactions 1–6) aimed at replenishing propionyl-CoA into CETCH cycle. The red box evidences the artificial wire CETCH + BHAC + (part of) serine cycle fixing CO_2 into acetyl-CoA. Reaction 1: propionyl-CoA carboxylase engineered to carboxylate acetyl-CoA to malonyl-CoA [37]; reactions 2 and 3: bifunctional malonyl-CoA/malonate semialdeide reductase [38]; reactions 4 and 5: propionyl-CoA synthase, a multicatalytic nanocompartment recently characterized [39]; reaction 6: propionyl-CoA synthase (for acrylyl-CoA reduction to propionyl-CoA). Absolute configurations of chiral centers are reported only if specified in the original source. (Previously unpublished Scheme).

Finally, with the use of the effective replenishing Module C, propionyl-CoA and methylmalonyl-CoA (both CETCH intermediates shown in Scheme 2) could be used to feed the synthesis of 6-deoxyerythronlide B (6-DEB, the macrolide backbone of erythromycin) through the DEBS Module, catalyzing the net reaction shown in Scheme 8.

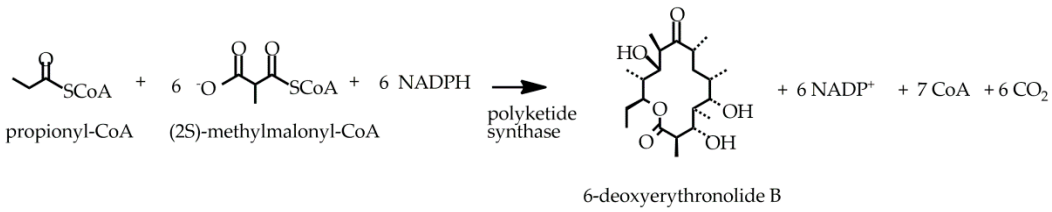

Scheme 8. Synthesis of 6-deoxyerythronolide B (6-DEB) by 6-deoxyerythronolide B synthase added to the artificial wire CETCH + BHAC + (part of) serine cycle + Module C.

Under optimized conditions (under the cofactors regeneration conditions), the complete set of 54 reactions produced 31.0 ± 1.6 μM of 6-DEB on glyoxylate supply (250 μM), allowing the calculation of a 172% yield in carbon conversion. It is important noting that the final carbon conversion yield reaches 172% (in comparison with methylmalonyl-CoA carbon conversion yield of 400%) as the synthesis of 6-deoxyerythronolide B produces 6 moles of CO_2.

To confirm the decisive positive effect of replenishing module C, testing the synthetic potential of the CETCH cycle alone + 6-DEB synthase did not result in 6-DEB synthesis.

4.3. Artificial Pathways Based on Enoyl-CoA Carboxylase Enzymes: The HOPAC Cycle

Very recently, the Erb Group implemented in vitro a synthetic cycle named HOPAC (Hydroxypropionyl-CoA/acrylyl-CoA) designed since 2016 [40]. The metabolite sequence of the cycle is very similar to the sequence of the 3-hydroxypropionyl-CoA pathway

studied in *Chloroflexus aurantiacus* [20]. However, the HOPAC cycle differs from the natural autotrophic pathway in some key reactions, and the native thermophilic enzymes from *Chloroflexus aurantiacus* have been replaced (whenever possible) by mesophilic alternatives, gathering eleven core enzymes from six different organisms.

Therefore, the HOPAC cycle, with the complete sequence of reaction shown in Scheme 9, can be considered a new-to-Nature CO_2-fixation cycle.

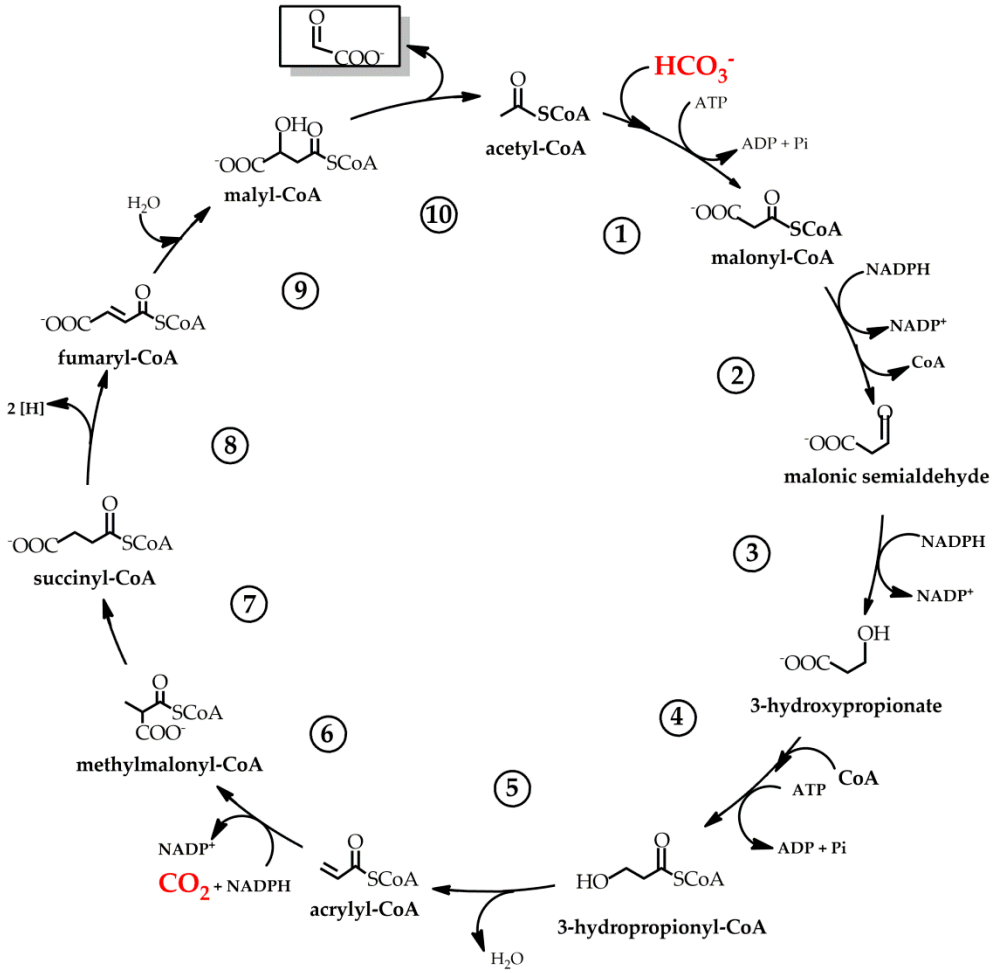

Scheme 9. The HOPAC cycle (version 4.0). Reaction 1: propionyl-CoA carboxylase; reaction 2 and 3: malonyl-CoA reductase; reaction 4: propionyl-CoA ligase; reaction 5: enoyl-CoA hydratase; reaction 6: crotony-CoA carboxylase; reaction 7 is catalyzed by two enzymes: methylmalonyl-CoA mutase and methylmalonyl-CoA epimerase; reaction 8: (2*S*)-methylsuccinyl-CoA deidrogenase; reaction 9: mesaconyl-CoA hydratase; reaction 10: malyl-CoA lyase. Reactions 2–6 are the reconstruction of the 3-OH propionate route. Reactions 7–10 are the reconstruction of the fumaryl route. Absolute configurations of chiral centers are reported only if specified in the original source. (Scheme from ref. [40], adapted and used from original source distributed under a Creative Commons Attribution Non-Commercial License 4.0).

The net stoichiometry of the HOPAC cycle is summarized in Equation (7).

$$2\,CO_2 + 3\,(NADPH + H^+) + 2\,ATP + FAD \rightarrow glyoxylate + 3\,NADP^+ + 2\,ADP + 2\,Pi + FADH_2 \quad (7)$$

It must be noted that, instead of propionyl-CoA used in the CETCH cycle, acetyl-CoA is used as molecular carrier (at concentration of 200 μM). The best-performing variant of the cycle (version 4.0) has the following features:

(1) the carboxylation of acetyl-CoA to malonyl-CoA (reaction 1) was effectively achieved by using a propionyl-CoA carboxylase from *Methylorubrum extorquens*, engineered through a D407I mutation to increase the selectivity towards acetyl-CoA;
(2) malonyl-CoA reductase from *Chloroflexus aurantiacus* catalyzes both the malonyl-CoA reduction to malonic semialdehyde (reaction 2) and the subsequent reduction of the semialdehyde to 3-hydroxypropionate (reaction 3);
(3) for the activation 3-hydroxypropionate to 3-hydroxypropionyl-CoA, a propionyl-CoA ligase from *Cupravidus necator* was selected (reaction 4);
(4) for the dehydration of 3-hydroxypropionyl-CoA to acrylyl-CoA, enoyl-CoA hydratase from *Pseudomonas aeruginosa* was chosen (reaction 5);
(5) acrylyl-CoA is carboxylated to methylmalonyl-CoA in a reductive carboxylation reaction by crotony-CoA carboxylase, an enoyl-CoA carboxylase/reductase from *Methylorubrum extorquens* (reaction 6).

The use of the engineered propionyl-CoA carboxylase from *Methylorubrum extorquens* (enoyl-CoA carboxylase/reductase) and the NADPH dependent crotony-CoA carboxylase exploits, similarly to the CETCH cycle, some of the most active enzyme in CO_2-fixation.

Scheme 10 compares the acrylyl-CoA carboxylation in the natural 3-hydroxypropionyl-CoA pathway (Scheme 10a) with the acrylyl-CoA reductive carboxylation to methylmalonyl-CoA (Scheme 10b) adopted in the HOPAC cycle. It can be noted that, in the natural autotrophic pathway, acrylyl-CoA is firstly reduced to propionyl-CoA and subsequently carboxylated to methylmalonyl-CoA in an ATP dependent reaction. In contrast, the acrylyl-CoA carboxylation of the HOPAC cycle avoids ATP (Scheme 10b) hydrolysis, resulting in approximately 33% more ATP-efficiency than natural 3-hydroxypropionate pathway.

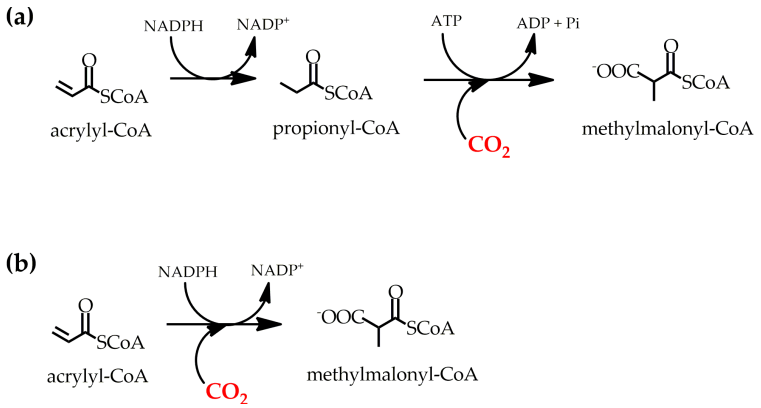

Scheme 10. Comparison of the carboxylation of acrylyl-CoA to methylmalonyl-CoA in the natural 3-hydroxypropionyl-CoA pathway from *Chloroflexus aurantiacus* (**a**) with the acrylyl-CoA carboxylation in the HOPAC cycle (**b**). In *Chloroflexus aurantiacus*, acrylyl-CoA is first reduced to propionyl-CoA and subsequently carboxylated to methylmalonyl-CoA in an ATP dependent reaction; in the HOPAC cycle, the synthesis of methylmalonyl-CoA is achieved by carboxylative reduction of acrylyl-CoA. Absolute configurations of chiral centers are reported only if specified in the original source (Previously unpublished Scheme).

The subsequent conversion of methylmalonyl-CoA into acetyl-CoA and glyoxylate (reactions 7–10 in Scheme 9) is considered the "oxidative part" of the cycle with respect to the "reductive part" (reactions 1–6).

Isomerization of methylmalonyl-CoA into succinyl-CoA (reaction 7) requires two enzymes (a mutase and a methylmalonyl-CoA epimerase), while a methylsuccinyl-CoA deidrogenase catalyzes the oxidation of succinyl-CoA to fumaryl-CoA (reaction 8).

Interestingly, the Authors have used a methylsuccinyl-CoA dehydrogenase from *Pseudomonas migulae*, which required the addition of an electron transfer protein (Etf + FAD cofactor) and a quinone reductase protein (EtfQ + quinone cofactor) to obtain efficient substrate oxidation coupled to O_2 reduction to H_2O_2. Finally, fumaryl-CoA is hydrated to

malyl-CoA from mesaconyl-CoA hydratase (reaction 9), and malyl-CoA is split into acetyl-CoA and glyoxylate by a malyl-CoA lyase (reaction 10) enzyme. Glyoxylate is ultimately reduced to glycolate by a glyoxylate reductase enzyme (not shown in Scheme 9) to drive the cycle forward.

Overall, after computer-aided optimization of the system by the METIS platform [41], a variant of the HOPAC cycle was established, producing approximately 1500 µM of glycolate starting from 200 µM of acetyl-CoA in approximately 2 h at a rate of 2.4 nmol of CO_2 min^{-1} mg^{-1} protein, thus comparing with the efficiency of the CETCH cycle.

4.4. Pathway Based on 6-Phosphogluconate Dehydrogenase Enzyme: The GED Cycle

An interesting work published by Bar-Even et al. in 2020 [42] aimed at constructing an artificial autothrophic CO_2-fixation pathway in *E. coli* gathering only endogenous enzymes of the heterotrophic bacteria. The study was part of an ambitious research line intended to adapt the heterotrophic bacterium to an autotrophic metabolism.

With the aid of genome-scale metabolic model [43], the Authors reconstructed in *E. coli* the GED (Gnd–Entner–Doudoroff) cycle, around the central carboxylase 6-phosphogluconate dehydrogenase (Gnd) enzyme, which catalyzes the reductive carboxylation of Ribulose-5-phosphate (Ru5P) to 6-phosphogluconate (Scheme 11). Subsequently, the GED cycle exploits several enzymes from the Entner–Doudoroff (ED) pathway (schematized in green box in Scheme 11), enzymes from gluconeogenesis (schematized in blue box in Scheme 11) and, finally, enzymes of the pentose phosphate pathway (schematized in red box in Scheme 11).

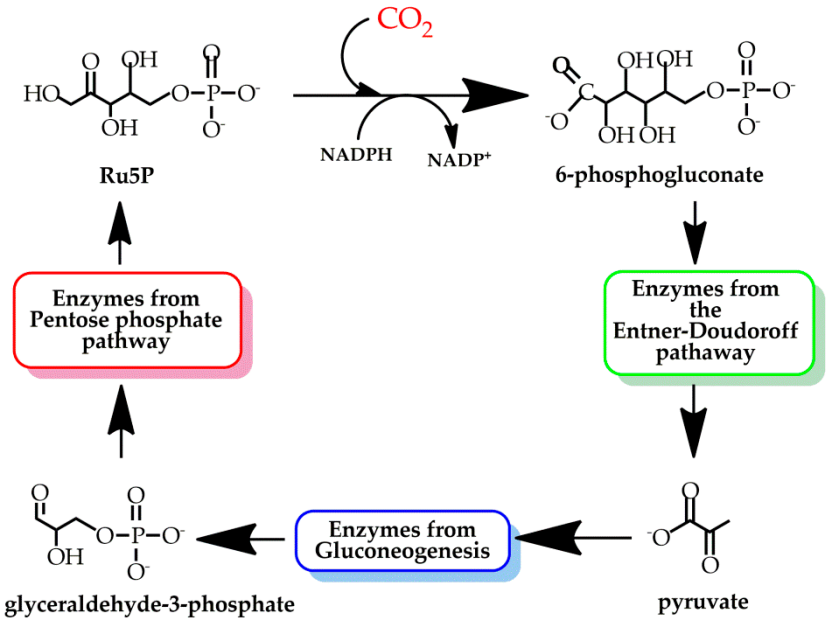

Scheme 11. The GED (Gnd–Entner–Doudoroff) cycle. 6-phosphogluconate (6PG) dehydrogenase converts RuBP into 6-phosphogluconate; enzymes in the green box belong to the Entner–Doudoroff cycle and converts 6-phosphogluconate into pyruvate. Enzymes in the blue box belong to the gluconeogenesis pathway. Glyceraldehyde-3-phosphate is converted into Ribulose-5-phosphate by enzymes from the pentose phosphate cycle (schematized in red box). (Previously unpublished Scheme).

The intermediate 6-phosphogluconate is dehydrated to 2-keto-3-deoxygluconate-6-phosphate, which splits into pyruvate and glyceraldehyde-3-phosphate (GA3P) by a 2-keto-3-deoxygluconate-6-phosphate aldolase. Pyruvate is activated to phosphoenolpyruvate and ultimately to 3-phosphoglycerate (3PG), prior to undergoing reduction to gliceraldehyde-3-phosphate (GA3P). The two GA3P units enter the pentose phosphate pathway being converted into Ru5P.

Any of the intermediates of the GED cycle can be diverted towards other biosynthetic routes, allowing easy integration with the bacterial metabolism. Taking pyruvate as the

molecular target of the cycle, the production of 1 mol of pyruvate (3 rounds of the GED cycle) requires 6 mol of ATP, while the CBB cycle requires 7 mol of ATP per pyruvate.

The cycle was successfully tested in vivo after over-expression of the key enzymes and small modifications of the endogenous metabolic network.

4.5. Pathways Constructed around Phosphoenolpyruvate Carboxylase (Pepc): MCG and rGS Pathways

Besides enoyl-CoA carboxylase/reductase enzymes, phosphoenolpyruvate carboxylase (Pepc) is one of the most active carboxylases with no oxygenase activity (Table 1).

The Liao Group has built a new synthetic cycle named malyl-CoA-glycerate (MCG, evidenced by red arrows in Scheme 12, reactions 1–8) functioning in tandem with a reductive Glyoxylate Synthesis (rGS, evidenced by blue arrows in Scheme 12, reactions 1–4) pathway, exploiting phosphoenolpyruvate carboxylase as the key CO_2-fixing enzyme [44]. The sequence of reactions of the rGS–MCG pathway is shown in Scheme 12, evidencing that the first four reactions of the MCG cycle are in common to the rGS pathway.

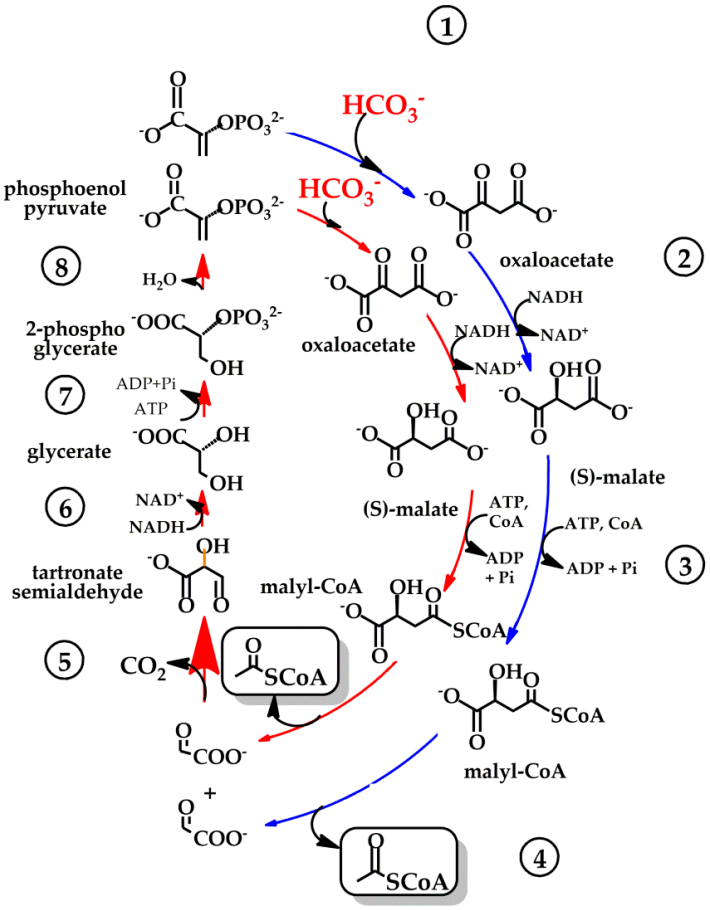

Scheme 12. The rGS–MCG pathway. Reactions evidenced by blue arrows construct the reductive Glyoxylate Synthesis (rGS) pathway. Reaction evidenced by red arrows construct the malyl-CoA-glycerate (MCG) pathway. Reaction 1: phosphoenolpyruvate carboxyloase (Pepc); reaction 2: malate dehydrogenase; reaction 3: malate thiokinase; reaction 4: malyl-CoA lyase; reaction 5: glyoxylate carboligase; reaction 6: tartronate semialdehyde reductase; reaction 7: glycerate kinase; reaction 8: enolase. According to the path stoichiometry, 2 mol of phosphoenolpyruvate enter the rGS–MCG pathway, and only 1 mol of phosphoenolpyruvate is regenerated at the end of the cycle. Absolute configurations of chiral centers are reported only if specified in the original source. (Scheme from ref. [44], adapted and used from original source distributed under the Creative Commons Attribution 4.0 International License, http://creativecommons.org/licenses/by/4.0/ (accessed on 23 September 2024)).

In the rGS–MCG cycle, formally 2 mol of Pep start the rGS and the MCG pathways, respectively, undergoing carboxylation to 2 mol of oxaloacetate, which is subsequently reduced to malate and activated to malyl-CoA. The malyl-CoA lyase enzyme splits the 2 mol of malyl-CoA into 2 mol of acetyl-CoA and 2 mol of glyoxylate.

As part of the MCG cycle, the 2 mol of glyoxylate undergo condensation into tartronate semialdehyde (1 mol), liberating one CO_2 molecule (reaction 5). Subsequent reactions typical of the bacterial glyoxylate assimilation route are needed for fosphoenolpyruvate (1 mol) regeneration from tartronate semialdehyde (reactions 6–8).

The net stoichiometry of the rGS–MCG cycle fed by phosphoenolpyruvate (Pep) allows the synthesis of 2 mol of acetyl-CoA starting from Pep and HCO_3^- according to Equation (8).

$$\text{Pep} + HCO_3^- + 2\ \text{HSCoA} + 3\ (\text{NADH} + H^+) + 3\ \text{ATP} \rightarrow 2\ \text{acetyl-CoA} + 3\ NAD^+ + 3\ \text{ADP} + 3\ \text{Pi} \quad (8)$$

However, the MCG cycle can alternatively be fed with glycolate (oxidized to glyoxylate before entering the cycle). Under these conditions, the rGS pathways does not operate, and the net stoichiometry of the reaction is shown in Equation (9).

$$\text{Glyoxylate} + \text{HSCoA} + \text{NADH} + H^+ + 2\ \text{ATP} \rightarrow \text{acetyl-CoA} + NAD^+ + 2\ \text{ADP} + 2\ \text{Pi} \quad (9)$$

Under these circumstances, the cycle does not fix CO_2 (1 mol of HCO_3^- is fixed into oxaloacetate, and 1 mol of CO_2 is liberated in reaction 5), but the cycle is suitable for the conversion of glyoxylate into acetyl-CoA without carbon loss, making it very useful when expressed in plants that suffer from leak of CO_2 through photorespiration.

The rGS–MCG cycle fed by Pep offers relatively easy integration into natural metabolic pathways as, in vivo, Pep is produced from natural metabolic routes (as for example glycolysis or the CBB cycle), and acetyl-CoA can enter various biosynthetic routes.

Interestingly, the rGS–MCG cycle was tested in vitro and expressed in vivo in both in *E. coli* and in *Synechocistis elongates* PCC7942 strain, showing optimal integration in living organisms.

In photosynthetic organisms, the native pathway converting Pep into acetyl-CoA is part of the CBB + PDH (pyruvate dehydrogenase enzyme) pathway shown in Scheme 13a, involving the conversion of 3-phospho-glycerate (3PGA, produced by the CBB cycle) into pyruvate and, ultimately, into acetyl-CoA by "losing" one CO_2 molecule.

According to the stoichiometry of reactions 1–4 in Scheme 13a, the synthesis of 1 mol of acetyl-CoA (a C2 compound) requires 1 mol of 3PGA (a C3 compound), which, in turn, is produced by fixation of 3 mol of CO_2 by the CBB cycle (in three subsequent rounds). Therefore, the theoretic yield of fixed carbon through this route is of 66% [C2/(3 × CO_2)].

On the contrary, considering the rGS–MCG cycle's integration with the CBB cycle (reactions 1–2 in Scheme 13b and Equation (8)), 1 mol of Pep (C3) and 1 mol of HCO_3^- are converted into 2 mol of acetyl-CoA (2 × C2). In this case, Pep is produced in a 1:1 mol ratio with respect to 3-phospho-D-glycerate, thanks to phosphoglycerate mutase and enolase enzymes. Therefore, the production of 2 mol of acetyl-CoA requires the fixation of 3 mol of CO_2 (three rounds of the CBB cycle) plus 1 mol of HCO_3^-, allowing for a theoretical carbon fixation yield of 100% [2 × C2/(3 × CO_2 + HCO_3^-)].

Therefore, linking the rGS + MGC cycle to the natural CBB cycle results in a more efficient carbon fixation yield, but also in a more efficient coenzymes exploitation if compared to the CBB + PDH natural pathway, as shown in Table 2.

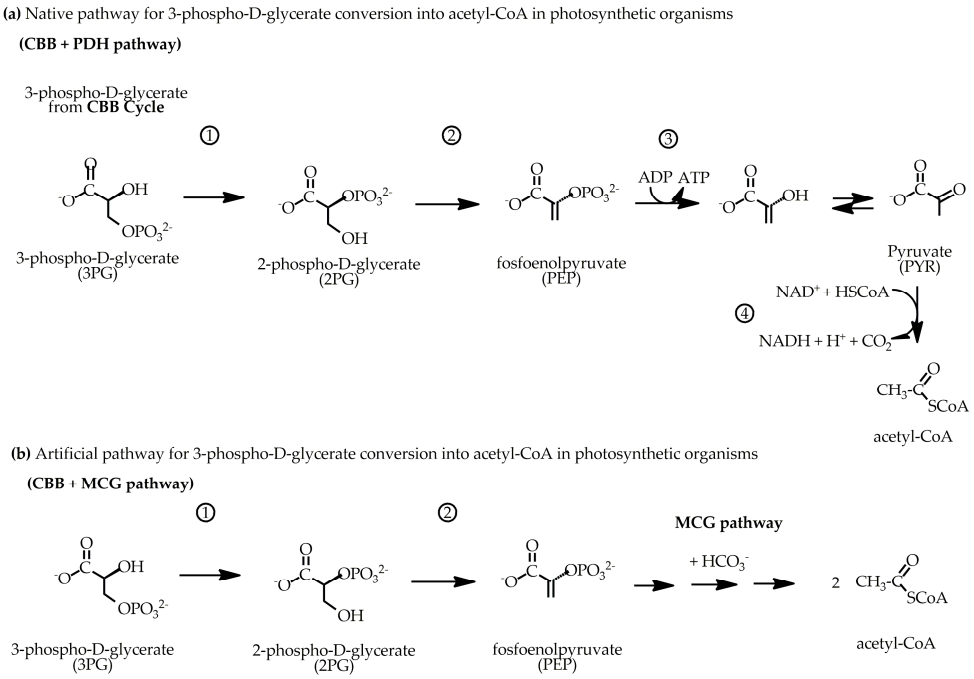

Scheme 13. Comparison of 3-phospho-D-glycerate conversion into acetyl-CoA in native photosynthetic organisms (**a**) and in artificial photosynthetic pathway connecting CBB cycle to MCG pathway (**b**). Reaction 1: phosphoglycerate mutase; reaction 2: enolase (phosphopyruvate hydratase); reaction 3: pyruvate kinase; reaction 4: pyruvate dehydrogenase. It can be noted that in (**b**) a phosphoglycerate mutase enzyme, converting 3PGA into 2-phospho-glycerate as precursor of PEP entering the MCG cycle, allows linking the artificial MCG cycle to natural CBB cycle with the synthesis of 2 mol of acetyl-CoA/1 mol of 3-phospho-D-glycerate. (Previously unpublished Scheme).

Table 2. Comparison of coenzyme requirements for the native CBB + PDH pathway and the artificial CBB + rGS + MCG pathway.

Entry 1: Native CBB + PDH pathway				
3 rounds of CBB cycle (i.e., 3 CO_2 fixation into 3PGA) feeding CBB + PDH cycles	$-CO_2$	4 NAD(P)H	7 ATP	to obtain 1 acetyl-CoA
Entry 2: linking artificial rGS + MCG cycle to natural CBB pathway				
3 rounds of CBB cycle (i.e., 3 CO_2 fixation into 3PGA) feeding rGS + MCG cycles	$+CO_2$	8 NAD(P)H	11 ATP	to obtain 2 acetyl-CoA
Entry 3: linking artificial rGS + MCG cycle to natural CBB pathway normalized to 1 mol of acetyl-CoA				
1.5 rounds of CBB cycle (i.e., 1.5 CO_2 fixation into 1.5 3PGA) feeding rGS + MCG cycles	$+½\ CO_2$	4 NAD(P)H	5.5 ATP	to obtain 1 acetyl-CoA

As a matter of fact, inspection of Entry 1 of Table 2 shows that the coenzyme requirements for the production of 1 mol of acetyl-CoA from the native CBB + PDH pathway are 4 mol of NAD(P)H and 7 mol of ATP. In comparison, after normalization to the production of 1 mol of acetyl-CoA (Entry 3 of Table 2), the CBB + rGS + MCG pathway requires 4 mol of NAD(P)H and 5.5 mol of ATP.

As referred to above, due to its relatively easy integration with the bacterial metabolism, the functionality of the rGS + MCG pathway could be demonstrated both in vitro and in vivo in *E. coli* and in *Synechococcus elongates* PCC7942 strain.

Expression of the complete set of rGS–MCG enzymes into *E. coli* allowed linking to the native glycolytic pathway (as phosphoenolpyruvate enters the rGS–MCG cycle), and transformed microorganisms produced acetyl-CoA and ethanol with high yield.

Moreover, integration of the complete set of genes coding for enzymes of the rGS–MCG cycle into the cyanobacteria *Synechococcus elongates* PCC7942 strain allowed linking of the rGS + MCG cycle to the CBB cycle, thanks to the reactions shown in Scheme 13b.

In the transgenic bacterial strain (grown under 50 mE s^{-1} m^{-2}), the measurement of intracellular acetyl-CoA levels and HCO_3^- consumption from the medium (charged with 50 mM of ^{13}C-labeleld HCO_3^-) almost doubled compared to wild strain, while the efficiency of the photosystems (measured by photosynthetic O_2 evolution) was unchanged. Consequently, it was concluded that the functioning of the new wire CBB + rGS + MCG pathways allows for increased efficiency of carbon fixation through a more efficient exploitation of coenzymes produced by the bacterial photosystems.

In summary, the cycles designed by the Liao Group (Schemes 12 and 13) pave the way for a more efficient conversion of CO_2 into acetyl-CoA, exploiting the activity of phosphoenolpyruvate carboxylase enzyme, one of the most robust and active carbon fixing enzymes, working "in addition to Rubisco". This also enables a more efficient biosynthesis of bio-products, with a potential for improvement of the bio-based economy.

4.6. Design and Implementation of Anapleurosis Pathway for the rGS + MCG Cycle

A further development of the rGS + MCG pathway was aimed at designing a cell-free CO_2-fixation pathway to achieve CO_2-fixation uncoupled from biomass production [45]. The reaction sequence designed (and implemented) by Liao and co-workers to feed phosphoenolpyruvate into rGS + MCG pathway is quite complex but very effective in CO_2-fixation and, in principle, scalable with enzyme concentration.

Liao et al. [45] pointed at constructing a self-replenishing cycle enabling pyruvate (a C3 compound) regeneration from part of the acetyl-CoA (a C2 compound) produced by the rGS pathway and CO_2, exploiting the high catalytic activity of crotonyl-CoA carboxylase/reductase. The replenishing pathway (evidenced by green arrows in Scheme 14) is named reductive Pyruvate Synthetic pathway (rPS) and embodies a sequence of eleven consecutive reactions (reactions 9–19 in Scheme 14). In the closing stage of the rPS pathway (reaction 19), phosphoenolpyruvate syntase converts pyruvate into Pep, so that the complete cycle resulting from integration of rGS + rPG pathways is named rGPS.

To obtain the net stoichiometry of the rGPS–MCG cycle, the following partial reactions (Equations (10)–(13)) have to be summed up.

Considering the stoichiometry of the reactions 1–4 in Scheme 14 (as part both of rGS and MCG pathways), 2 mol of Pep are converted into 2 mol of acetyl-CoA and 2 mol of glyoxylate according to Equation (10):

$$2\ \text{Pep} + 2\ HCO_3^- + 2\ (\text{NADH} + H^+) + 2\ \text{HSCoA} + 2\ \text{ATP} \rightarrow 2\ \text{acetyl-CoA} + 2\ \text{glyoxylate} + 2\ NAD^+ + 2\ \text{ADP} + 2\ \text{Pi} \quad (10)$$

When Equation (10) is summed up with Equation (11) (summarizing the stoichiometry of the glyoxylate assimilation pathway, reactions 5–8 of Scheme 14), Equation (12) (summarizing the stoichiometry of the reductive Pyruvate Synthesis, reactions 9–18 of Scheme 14), and Equation (13) consisting in pyruvate conversion into phosphoenolpyruvate (reaction 19, Scheme 14):

$$2\ \text{glyoxylate} + (\text{NADH} + H^+) + \text{ATP} \rightarrow \text{Pep} + CO_2 + NAD^+ + \text{ADP} + \text{Pi} \quad (11)$$

$$\text{acetyl-CoA} + CO_2 + (\text{NADH} + H^+) + (\text{NADPH} + H^+) + \text{FAD} \rightarrow \text{pyruvate} + NAD^+ + NADP^+ + FADH_2 + \text{HSCoA} \quad (12)$$

$$\text{pyruvate} + \text{ATP} \rightarrow \text{Pep} + \text{AMP} + \text{PPi} \quad (13)$$

the overall stoichiometry of the self-replenishing rGPS + MCG cycle is given in Equation (14), resulting in the synthesis of acetyl-CoA directly from CO_2:

$$2\ HCO_3^- + 4\ ATP + (NADPH + H^+) + 4\ (NADH + H^+) + FAD + HSCoA \rightarrow \text{acetyl-CoA} + 3\ ADP + 3\ Pi + AMP + PPi + NADP^+ + 4\ NAD^+ + FADH_2 \quad (14)$$

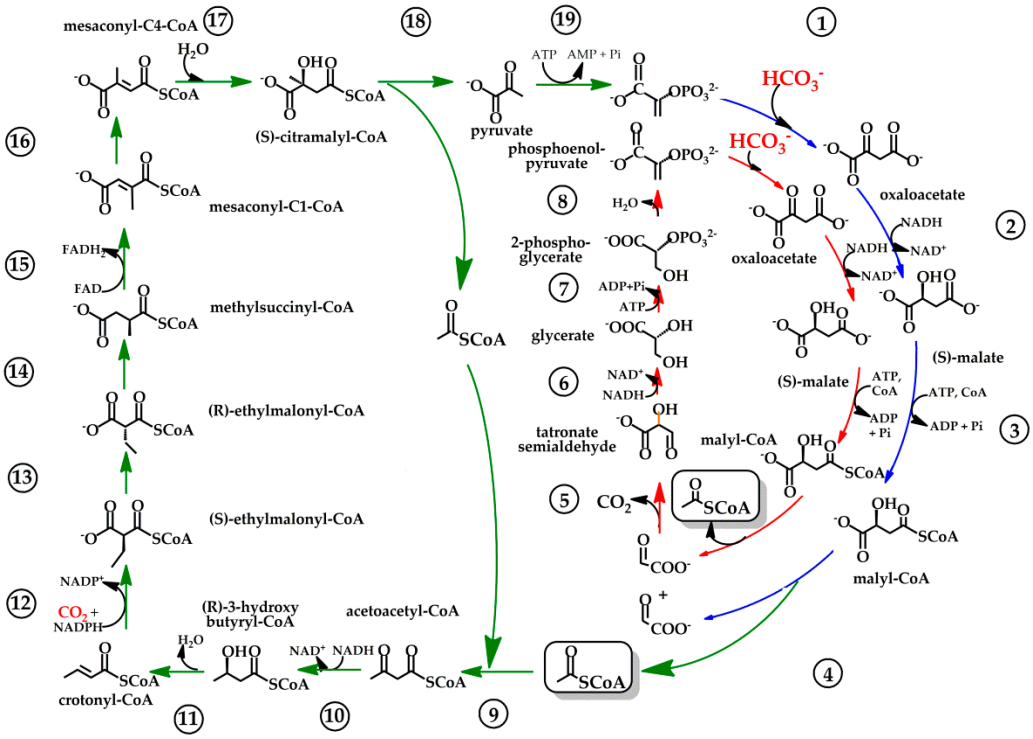

Scheme 14. The rGPS–MCG cycle producing acetyl-CoA from CO_2. The rGPS cycle consists of the rGS pathway (evidenced by blue arrows) and the replenishing rPS pathway (evidenced by green arrows). The MCG pathway is evidenced by red arrows. Reactions 1–8 are catalyzed by enzymes shown in Scheme 12. Reaction 9: acetyl-CoA acetyltransferase; reaction 10: 3-hydroxybutyryl-CoA dehydrogenase; reaction 11: crotonase; reaction 12: crotonyl-CoA carboxylase/reductase; reaction 13: ethylmalonyl-CoA epimerase; reaction 14: (2*R*)-ethylmalonyl-CoA mutase; reaction 15: (2*S*)-methylsuccinyl-CoA dehydrogenase; reaction 16: mesaconyl-C1-CoA-C4-CoA transferase; reaction 17: mesaconyl-C4-CoA hydratase; reaction 18: (*S*)-citramalyl-CoA lyase; reaction 19: phosphoenolpyruvate synthetase. Absolute configurations of chiral centers are reported only if specified in the original source. (Scheme from ref. [45], adapted and used from original source distributed under the Creative Commons Attribution 4.0 International License, http://creativecommons.org/licenses/by/4.0/ (accessed on 23 September 2024).

It can be noted that experimentally, the cycle is fed by crotonyl-CoA (0.4 mM) and Pep (0.4 mM), obtaining, after 6 h monitoring, acetyl-CoA (0.7 mM), pyruvate (0.4 mM), and malate (1 mM). Therefore, the self-replenishing property of the cycle allows the synthesis not only of acetyl-CoA but also of pyruvate and malate.

Some important notes have to be added about the synthetic strategy adopted by the rPS pathway (evidenced by green arrows in Scheme 14). The opening stage of the pathway (reaction 9) consists in the condensation of 2 acetyl-CoA units into acetoacetyl-CoA, while Equation (12) shows that the overall stoichiometry of the rPS pathway is the carboxylation of acetyl-CoA to pyruvate.

It could be argued that the shortest way to carboxylate acetyl-CoA to pyruvate would be the reductive carboxylation of acetyl-CoA catalyzed by pyruvate:ferredoxin oxidoreductase (PFOR) enzymes (Equation (15)):

$$\text{Acetyl-CoA} + CO_2 + 2\,e^- \rightarrow \text{pyruvate} + \text{HSCoA} \quad (15)$$

Unfortunately, to promote this reaction, a redox partner with an E°′ of approximately −500 mV is required, which is usually performed in vivo by ferredoxins. Neither NADH nor NADPH (E°′ = −320 mV) are available for acetyl-CoA carboxylative reduction in one step.

To circumvent this problem, the Liao Group has designed the sequence of favourable thermodynamic reactions shown in Scheme 14, starting with condensation of 2 acetyl-CoA units into acetoacetyl-CoA and subsequent reduction to (*R*)-3-hydroxybutyryl-CoA, assisted by NADH oxidation. The latter substrate, after dehydration, gives crotonyl-CoA, which is reductively carboxylated to (*S*)-ethylmalonyl-CoA with NADPH. Having consumed two moles of NAD(P)H + H^+, the "excess" of reduction potential is recovered three steps later with dehydrogenation of methylsuccinyl-CoA to mesaconyl-CoA, coupled with FAD reduction to $FADH_2$ by the (2*S*)-methylsuccinyl-CoA dehydrogenase enzyme.

Most part of enzymes collected into the rGPS cycle were selected from different bacteria; their genes were cloned, expressed in *E. coli*, and proteins were purified. Only phosphoenolpyruvate carboxylase, malate dehydrogenase, and enolase were commercially available.

Obviously, the rGPS–MCG cycle functioning (according to Equation (14)) requires cofactor regeneration, which was accomplished by adding formate and formate dehydrogenase for NADH regeneration according to the reverse of Equation (3) (analogous to the CETCH cycle).

In contrast, for NADPH and ATP regeneration, different enzymes with respect to CETCH and HOPAC cycle were implemented. NADPH was regenerated by adding glucose-6-phosphate and glucose-6-phosphate dehydrogenase according to Equation (16), and ATP was regenerated by adding creatine phosphate and creatine kinase according to Equation (17).

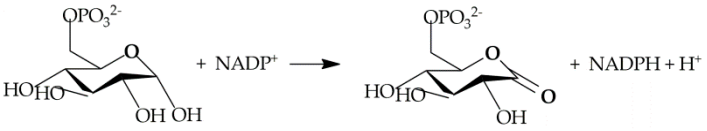

(16)

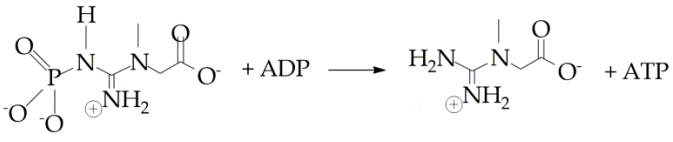

(17)

To ensure the cycle operates continuously, FAD regeneration from $FADH_2$ was also needed. This was achieved oxidizing $FADH_2$ with ferrocenium (Fc^+) as an artificial electron acceptor. Ultimately, reduced ferrocene (Fc) could be oxidized using electrochemical approach or horseradish peroxidase Hrp/H_2O_2 system, as shown in Scheme 15. The latter strategy proved to be more effective within the cell-free system.

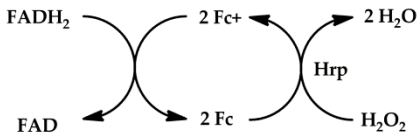

Scheme 15. $FADH_2$ reoxidation within the rGPS+MCG cycles. Hrp is horseradish peroxidise enzyme.

Moreover, it was necessary to adopt complex regulation circuits to maintain optimal concentrations of substrates and coenzymes. The concentration of coenzymes, Fc^+, and

H_2O_2 were constantly monitored via an opto-sensing module and all concentrations were maintained at their optimum values, achieving a "quasi-steady-state" operation conditions for 6 h.

This allowed for a specific CO_2 fixation rate of 28.5 nmol of CO_2 min^{-1} mg^{-1} of core proteins for the system, having reached a quasi-steady-state. These data exceed the CO_2 fixation rate of the CETCH (5.4 version) cycle and are comparable with the specific CO_2-fixation rate of several photosynthetic bacteria.

4.7. Pathway Constructed around Crotonyl-CoA Carboxylase/Reductase and Phosphoenopyruvate Carboxylase: The THETA Cycle

Very recently, Erb et al. [46] have designed and implemented in vitro a new-to-Nature CO_2-fixation pathway, constructed around two of the most active carboxylase enzymes: the phosphoenopyruvate carboxylase (Pepc) and crotonyl-CoA carboxylase/reductase enzymes (Ccr). The cycle gathers 17 enzymes from 8 different organisms and has been named THETA cycle (from reductive tricarboxylic acid branch/4-hydroxybutyryl-CoA/ethylmalonyl-CoA/acetyl-CoA), with the sequence of metabolites shown in Scheme 16.

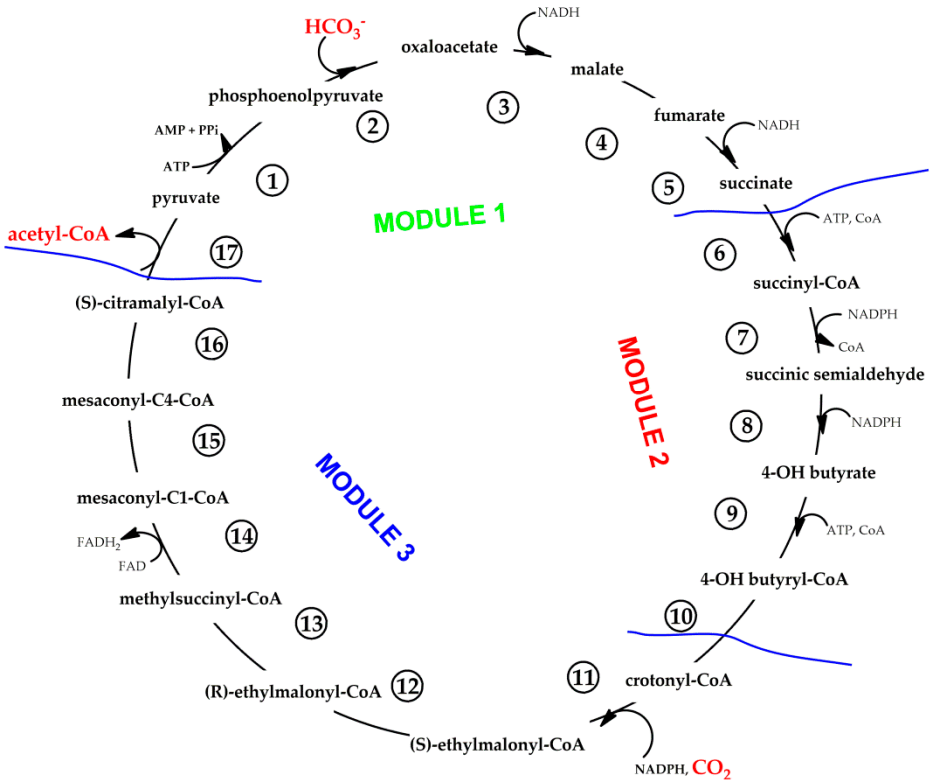

Scheme 16. Sequence of metabolites of the THETA cycle. Reaction 1: phosphoenolpyruvate synthase; reaction 2: phosphoenolpyruvate carboxylase; reaction 3: malate dehydrogenase; reaction 4: fumarase; reaction 5: fumarate reductase (NADH); reaction 6: succinyl-CoA ligase; reaction 7: succinyl-CoA reductase; reaction 8: succinic semialdehyde reductase; reaction 9: 4-hydroxybutyryl-CoA synthase; reaction 10: 4-hydroxybutyryl-CoA dehydratase; reaction 11: crotonyl-CoA carboxylase/reductase; reaction 12: ethylmalonyl-CoA epimerase; reaction 13: (2R)-ethylmalonyl-CoA mutase; reaction 14: methylsuccinyl-CoA oxidase; reaction 15: mesaconyl-C1-CoA-C4-CoA transferase; reaction 16: mesaconyl-C4-CoA hydratase; reaction 17: (S)-citramalyl-CoA lyase. The complete cycle can be divided in three modules: Module 1 converting pyruvate into succinate, Module 2 converting succinate into 4-OH butyryl-CoA, and Module 3 converting 4-OH butyryl-CoA into pyruvate. (Scheme from ref. [46], adapted and used from original source distributed under the Creative Commons Attribution 4.0 International License, http://creativecommons.org/licenses/by/4.0/ (accessed on 23 September 2024).

The cycle was identified through a computational approach by Löwe et al. [47] in 2021 under the name citramalyl-CoA cycle and subsequently implemented in vitro by the Erb Group.

The overall stoichiometry of the cycle is summarized in Equation (18), evidencing the synthesis of acetyl-CoA from CO_2:

$$CO_2 + HCO_3^- + 4\ ATP + 3\ (NADPH + H^+) + 2\ (NADH + H^+) + FAD + HSCoA \rightarrow \text{acetyl-CoA} + 3\ NADP^+ + 2\ NAD^+ + 4\ ADP + 4\ Pi + FADH_2 \quad (18)$$

After optimizing the reaction sequence and the complex system by the METIS platform [39], the cycle allows for the synthesis of acetyl-CoA from CO_2 and HCO_3^- using pyruvate to start the cycle, reaching in vitro a CO_2-fixation rate of 2.7 nmol min^{-1} mg^{-1} of core proteins, which is very close to CO_2-fixation rate of the CBB cycle. Scheme 16 shows the cycle can be considered as composed of three modules: Module 1 converting pyruvate into succinate, Module 2 converting succinate into 4-OH butyryl-CoA, and Module 3 converting 4-OH butyryl-CoA into pyruvate. Each module was successfully implemented in vivo in transformed *E. coli* cells, paving the way to in vivo implementation of the cycle.

4.8. Pathway Constructed around Pyruvate:Ferredoxin Oxidoreductase: The POAP Cycle

Very recently, Li and co-workers have published a very short cycle named POAP, encompassing only four enzymes: pyruvate carboxylase, oxaloacetate acetylhydrolase, acetate-CoA ligase, and pyruvate synthase [48].

The reaction sequence of POAP cycle is shown in Scheme 17.

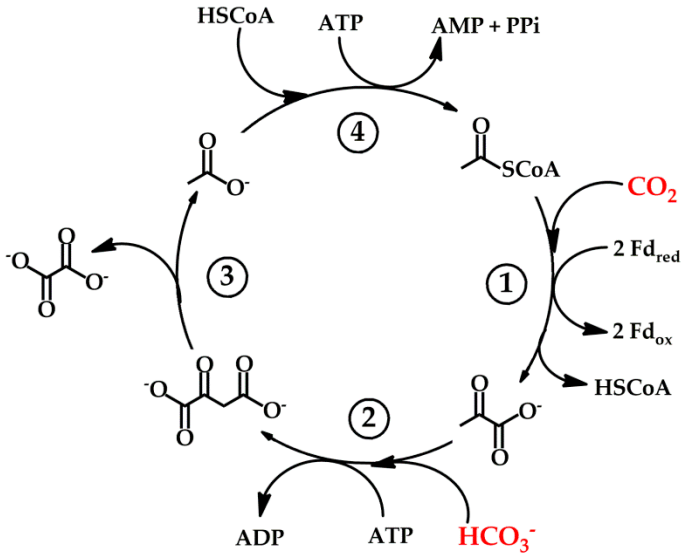

Scheme 17. The POAP cycle. Reaction 1: PFOR catalyzing acetyl-CoA carboxylation to pyruvate; reaction 2: pyruvate carboxylase; reaction 3: oxaloacetate acetylhydrolase; reaction 4: acetate-CoA ligase. (Scheme from ref. [48], adapted and used by permission of ACS (copyright© 2022)).

As noted in Section 4.6 carboxylation of acetyl-CoA to pyruvate (shown in Equation (15)) is a key reaction that could be obtained reverting the thermodynamically favourable oxidative decarboxylation of pyruvate, catalyzed by pyruvate ferredoxin oxidoreductase (PFOR, $\Delta rG'^m$ around -18 kJ mol^{-1}). In catalyzing the pyruvate decarboxylation, PFOR enzymes require thiamine pyrophosphate (TPP) as a cofactor and a ferredoxin (Fd) as a redox partner, as electrons are released at a $E^{\circ\prime}$ of around -540 mV [49]. Usually, anoxic conditions and high temperature are also required.

Li et al. [48] managed to use PFOR from *Clostridium thermocellum* and ferredoxin from *Hydrogenobacter thermophilus* ($E^{\circ\prime} = -500$ mV) selected as the optimal enzyme and redox

partner to catalyze the thermodynamic unfavourable acetyl-CoA carboxylation at 50 °C, under anaerobic conditions.

In reaction 2 of Scheme 17, pyruvate is further carboxylated to oxaloacetate, which is then split into oxalate and acetate. Finally, acetate activation into acetyl-CoA closes the cycle with favourable thermodynamics.

Enzymes catalyzing reactions 2–4 of Scheme 17 were selected from different bacteria: pyruvate carboxylase from *Geobacillus stearothermophilus*, oxaloacetate acetylhydrolase from *Aspergillus niger*, and acetate-CoA ligase from *Methanothrix thermoacetophila* respectively. Among these enzymes, oxaloacetate acetylhydrolase from *Aspergillus niger* showed sensitivity to the operational temperature (50 °C) and required replenishing during cycle operation.

The net stoichiometry of the POAP cycle is summarized in Equation (19), evidencing the synthesis of oxalate from CO_2:

$$2\ CO_2 + 2\ ATP + (NAD(P)H + H^+) \rightarrow \text{oxalate} + ADP + Pi + AMP + PPi + NAD(P)^+ \quad (19)$$

The cycle achieved a CO_2 fixation rate of 8.0 nmol of CO_2 min^{-1} mg^{-1} of proteins CO_2-fixing enzymes after 20 min at 50 °C. It can be noted that the complete cycle results to be highly active despite the thermodynamic unfavourable pyruvate carboxylation reaction. However, practical difficulties in implementing synthetic procedures arise because of the required operative conditions. The Authors propose that the constructed anaerobic cycle could be close to archaeal cycles that evolved under anaerobic conditions in earlier microorganisms.

5. Discussion and Perspectives

The previous survey evidences that great advances have been achieved over the last decade in order to set artificial reaction pathways for CO_2 fixation that rival in efficiency of known natural autotrophic fixation pathways [20].

If performed in in vitro experiment, artificial pathways can run only if NADH, ATP, and additional cofactors are adequately regenerated, and key metabolites are suitable by replenishing pathways.

To solve this problem, two following strategies can be implemented: (i) in vitro systems can be coupled to photosynthetic membranes (merging to the research area pointing to building of artificial cells); (ii) the artificial cycles are integrated in transformed microorganisms (both *E. coli* and photosynthetic microorganisms), thus coupling the artificial cycles to the cell energy metabolism.

Considering in vitro systems, other options would be photochemical NADH regeneration, which is usually implemented in hybrid systems (not subject of this review).

From an industrial biotechnology view, the research developed over the last decade takes a step forward in designing and implementing "as you desire" new synthetic routes gathering enzymes from different organisms, allowing for the down-selection of the most profitable processes concerning Carbon and Energy Efficiency.

Industrial biotechnology has decadal experience using gas-fermenting microorganisms for the production of chemicals requiring carbon supply in the form of CH_4, CO, or CO_2 with H_2 usually required for energy supply to the process. The latter is manly taken from syngas or waste treatment and is used in the synthesis of valuable chemicals as acids, alcohols, diols, aromatics, dienes, esters, ketones, and terpenes.

The artificial cycles discussed above have been constructed to synthesize intermediates as glyoxylate, acetyl-CoA, or oxalate, which can be connected to native biochemical wires for the synthesis of a wide range of target chemicals. In this way, industrial biotechnology is provided with a novel straightforward tool to manipulate microorganism metabolism, enabling the use of transformed gas-fermenting bacteria or photosynthetic microorganisms fed only by CO_2, with a metabolism "tailored" to produce target chemical.

Moreover, great industrial advance could also derive when artificial cycles are used in "cell free" factories. In this case, significant advantages come from: (i) production of target chemicals with energy supply coming from photosynthetic membranes or hybrid systems;

(ii) testing of thousands of different pathways in short time and process optimization guided by machine learning algorithm; (iii) focusing on the production of the target product while avoiding the grow of useless biomass.

6. Conclusions

According to the survey reported above, energy efficient pathways can be constructed and integrated in vivo into other natural biosynthetic wires, driving the synthesis of target metabolites entirely from CO_2.

This research field will probably find further development in the near future, with great potential to promote advances in the circular economy.

Funding: The University of Bari Aldo Moro is acknowledged for its financial support (Fondi di Ateneo).

Data Availability Statement: No new data were created or analyzed in this study.

Conflicts of Interest: The author declares no conflict of interest.

References

1. Hepburn, C.; Adlen, E.; Beddington, J.; Carter, E.A.; Fuss, S.; Mac Dowell, N.; Minx, J.C.; Smith, P.; Williams, C.K. The technological and economic prospects for CO_2 utilization and removal. *Nature* **2019**, *575*, 87–97. [CrossRef] [PubMed]
2. Xu, X.; Chen, D. Estimating global gross primary production based on satellite-derived phenology and maximal carbon uptake capacity. *Environ. Res.* **2024**, *252*, 119063. [CrossRef] [PubMed]
3. Schada von Borzyskowski, L.; Rosenthal, R.G.; Erb, T.J. Evolutionary history and biotechnological future carboxylases. *J. Biotechnol.* **2013**, *168*, 243–251. [CrossRef]
4. Thauer, R.K.; Kaster, A.-K.; Seedorf, H.; Buckel, W.; Hedderich, R. Methanogenic arcaea: Ecologically relevant differences in Energy conservation. *Nat. Rev. Microbiol.* **2008**, *6*, 576–591. [CrossRef]
5. Liu, Z.; Wang, K.; Chen, Y.; Tan, T.; Nielsen, J. Third-generation biorefineries as the means to produce fuels and chemicals from CO_2. *Nat. Catal.* **2020**, *3*, 274–288. [CrossRef]
6. Available online: https://www.oakbiosciences.com/technology/ (accessed on 23 September 2024).
7. Segraves, E.; Nelson, R. *Conversion of Industrial CO_2 Emission into Biofules and Chimica*; CCEMC Grand Challenge Round 1, Second Interim Report; OAKBIO—Tabita Lab: CCEMC Project #K130097; CCEMC: Stockton, CA, USA, 2015.
8. Peplow, M. The race to recycle carbon dioxide. *Nature* **2022**, *603*, 780–783. [CrossRef]
9. Stephanopoulos, G. Synthetic biology and metabolic engineering. *ACS Synth. Biol.* **2012**, *1*, 514–525. [CrossRef]
10. Bierbaumer, S.; Nattermann, M.; Schulz, L.; Zschoche, R.; Erb, T.J.; Winkler, C.K.; Tinzl, M.; Glueck, S.M. Enzymatic Conversion of CO_2: From natural to artificial utilization. *Chem. Rev.* **2023**, *123*, 5702–5754. [CrossRef]
11. Ünlü, A.; Ozdamar, Z.E.D.; Çaloğlu, B.; Binay, B. Enzymes for efficient CO_2 conversion. *Protein J.* **2021**, *40*, 489–503. [CrossRef]
12. Intasian, P.; Prakinee, K.; Phintha, A.; Trisrivirat, D.; Weeranoppanant, N.; Wongnate, T.; Chaiyen, P. Enzymes, in vivo biocatalysis, and metabolic engineering for enabling a circular economy and sustainability. *Chem. Rev.* **2021**, *121*, 10367–10451. [CrossRef]
13. Correa, S.S.; Schultz, J.; Lauersen, K.J.; Rosado, A.S. Natural carbon fixation and advances in synthetic engineering for redesigning and creating new fixation pathways. *J. Adv. Res.* **2023**, *47*, 75–92. [CrossRef] [PubMed]
14. Bernhardsgrutter, I.; Stoffel, G.M.M.; Miller, T.E.; Erb, T.J. CO_2-converting enzymes for sustainable biotechnology: From mechanisms to application. *Curr. Opin. Biotechnol.* **2021**, *67*, 80–87. [CrossRef] [PubMed]
15. Aleku, G.A.; Roberts, G.W.; Titchiner, G.R.; Leys, D. Synthetic enzyme-catalyzed CO_2 fixation reactions. *ChemSusChem* **2021**, *14*, 1781–1804. [CrossRef]
16. Nisar, A.; Khan, S.; Hameed, M.; Nisar, A.; Ahmad, H.; Mehmood, S.A. Bio-conversion of CO_2 into biofuels and other value-added chemicals via metabolic engineering. *Microbiol. Res.* **2021**, *251*, 126813. [CrossRef]
17. Erb, T.J. Photosynthesis 2.0: Realizing New-to-Nature CO_2-Fixation to Overcome the Limits of Natural Metabolism. *Cold Spring Harb. Perspect. Biol.* **2024**, *16*, a041669. [CrossRef]
18. Chen, P.-R.; Xig, P.-F. Carbon recycling with synthetic fixation pathways. *Curr. Opin. Biotechnol.* **2024**, *85*, 103023. [CrossRef]
19. Schulz-Mirbach, H.; Dronsella, B.; He, H.; Erb, T.J. Creating new-to-nature carbon fixation: A guide. *Metab. Eng.* **2024**, *82*, 12–28. [CrossRef] [PubMed]
20. Fuchs, G. Alternative pathways of carbon dioxide fixation: Insights into the early evolution of Life? *Annu. Rev. Microbiol.* **2011**, *65*, 631–658. [CrossRef]
21. Kim, S.; Lindner, S.N.; Aslan, S.; Yishai, O.; Wenk, S.; Schann, K.; Bar-Even, A. Growth of *E. coli* on formate and methanol via the reductive glycine pathway. *Nat. Chem. Biol.* **2020**, *16*, 538–545. [CrossRef]
22. Claassens, N.J.; Bordanaba-Florit, G.; Cotton, C.A.R.; De Maria, A.; Finger-Bou, M.; Friedeheim, L.; Giner-Laguarda, N.; Munar-Palmer, M.; Newell, W.; Scarinci, G.; et al. Replacing the Calvin cycle with the reductive glycine pathway in *Cupriavidus necator*. *Metab. Eng.* **2020**, *62*, 30–41. [CrossRef]

23. Hea, H.; Höpera, R.; Dodenhöfta, M.; Marlièreb, P.; Bar-Even, A. An optimized methanol assimilation pathway relying on promiscuous formaldehyde-condensing aldolases in *E. coli*. *Metab. Eng.* **2020**, *60*, 1–13. [CrossRef] [PubMed]
24. Cai, T.; Sun, H.; Qiao, J.; Zhu, L.; Zhang, F.; Zhang, J.; Tang, Z.; Wei, X.; Yang, J.; Yuan, Q.; et al. Cell-free chemo-enzymatic starch synthesis from carbon dioxide. *Science* **2021**, *373*, 1523–1527. [CrossRef] [PubMed]
25. Siegel, J.B.; Lee Smith, A.; Poust, S.; Wargacki, A.J.; Bar-Even, A.; Louw, C.; Shen, B.W.; Eiben, C.B.; Tran, H.M.; Noor, E.; et al. Computational protein design enables a novel one-carbon assimilation pathway. *Proc. Natl. Acad. Sci. USA* **2015**, *112*, 3704–3709. [CrossRef]
26. Lu, X.; Liu, Y.; Yang, Y.; Wang, S.; Wang, Q.; Wang, X.; Yan, Z.; Cheng, J.; Liu, C.; Yang, X.; et al. Constructing a synthetic pathway for acetylcoenzyme A from one-carbon through enzyme design. *Nat. Commun.* **2019**, *10*, 1378. [CrossRef]
27. Way, J.C.; Collins, J.J.; Keasling, J.D.; Silver, P.A. Integrating biological redesign: Where synthetic biology came from and where it needs to go. *Cell* **2014**, *157*, 151–161. [CrossRef]
28. Erb, T.J.; Jones, P.R.; Bar-Even, A. Synthetic metabolism: Metabolic engineering meets enzyme design. *Curr. Opin. Chem. Biol.* **2017**, *37*, 56–62. [CrossRef] [PubMed]
29. Bar-Even, A.; Noor, E.; Lewis, N.E.; Milo, R. Design and analysis of synthetic carbon fixation Pathways. *Proc. Natl. Acad. Sci. USA* **2010**, *107*, 8889–8894. [CrossRef]
30. Bar-Even, A.; Elad Noor, E.; Milo, R. A survey of carbon fixation pathways through a quantitative lens. *J. Exp. Bot.* **2012**, *63*, 2325–2342. [CrossRef]
31. Schwander, T.; Schada von Borzyskowski, L.; Burgener, S.; Socorro Cortina, N.; Erb, T.J. A synthetic pathway for the fixation of carbon dioxide in vitro. *Science* **2016**, *354*, 900–904. [CrossRef]
32. Erb, T.J.; Berg, I.A.; Brecht, V.; Muller, M.; Fuchs, G.; Alber, B.E. Synthesis of C5-dicarboxylic acids from C2-units involving crotonyl-CoA carboxylase/reductase: The ethylmalonyl-CoA pathway. *Proc. Natl. Acad. Sci. USA* **2007**, *104*, 10631–10636. [CrossRef]
33. Erb, T.J.; Brecht, V.; Fuchs, G.; Muller, M.; Alber, B.E. Carboxylation mechanism and stereochemistry of crotonyl-CoA carboxylase/reductase, a carboxylating enoyl-thioester reductase. *Proc. Natl. Acad. Sci. USA* **2009**, *106*, 8871–8876. [CrossRef] [PubMed]
34. Miller, T.E.; Beneyton, T.; Schwander, T.; Diehl, C.; Girault, M.; McLean, R.; Chotel, T.; Claus, P.; Socorro Cortina, N.; Baret, J.-C.; et al. Light-powered CO_2 fixation in a chloroplast mimic with natural and synthetic parts. *Science* **2020**, *368*, 649–654. [CrossRef] [PubMed]
35. Sundaram, S.; Diehl, C.; Socorro Cortina, N.; Bamberger, J.; Paczia, N.; Erb, T.J. A modular in vitro platform for the production of terpenes and polyketides from CO_2. *Angew. Chem. Int. Ed.* **2021**, *60*, 16420–16425. [CrossRef] [PubMed]
36. Diehl, C.; Gerlinger, P.D.; Paczia, N.; Erb, T.J. Synthetic anaplerotic modules for the direct synthesis of complex molecules from CO_2. *Nat. Chem. Biol.* **2023**, *19*, 168–175. [CrossRef]
37. Schwander, T. The Design and Realization of Synthetic Pathways for the Fixation of Carbon Dioxide In Vitro. Ph.D. Thesis, Philipps-Universität Marburg, Marburg, Germany, 2017.
38. Hügler, M.; Menendez, C.; Schägger, H.; Fuchs, G. Malonyl-Coenzyme a reductase from *Chloroflexus aurantiacus*, a key enzyme of the 3-Hydroxypropionate cycle for autotrophic CO_2 fixation. *J. Bacteriol.* **2002**, *184*, 2404–2410. [CrossRef]
39. Son, H.F.; Kim, S.; Seo, H.; Hong, J.; Lee, D.; Jin, K.S.; Park, S.; Kim, K.-J. Structural insight into bi-functional malonyl-CoA reductase. *Environ. Microbiol.* **2020**, *22*, 752–765. [CrossRef]
40. McLean, R.; Schwander, T.; Diehl, C.; Socorro Cortina, N.; Paczia, N.; Zarzycki, J.; Erb, T.J. Exploring alternative pathways for the in vitro establishment of the HOPAC cycle for synthetic CO_2 fixation. *Sci. Adv.* **2023**, *9*, eadh4299. [CrossRef]
41. Pandi, A.; Diehl, C.; Kharrazi, A.Y.; Scholz, S.A.; Bobkova, E.; Faure, L.; Nattermann, M.; Adam, D.; Chapin, N.; Foroughijabbari, Y.; et al. A versatile active learning workflow for optimization of genetic and metabolic networks. *Nat. Commun.* **2022**, *13*, 3876. [CrossRef]
42. Satanowski, A.; Dronsella, B.; Noor, E.; Vögeli, B.; He, H.; Wichmann, P.; Erb, T.J.; Lindner, S.N.; Bar-Even, A. Awakening a latent carbon fixation cycle in *Escherichia coli*. *Nat. Commun.* **2020**, *11*, 5812. [CrossRef]
43. Monk, J.M.; Lloyd, C.J.; Brunk, E.; Mih, N.; Sastry, A.; King, Z.; Takeuchi, R.; Nomura, W.; Zhang, Z.; Mori, H.; et al. *i*ML1515, a knowledgebase that computes *Escherichia coli* traits. *Nat. Biotechnol.* **2017**, *35*, 904–908. [CrossRef]
44. Yu, H.; Li, X.; Duchoud, F.; Chuang, D.S.; Liao, J.C. Augmenting the Calvin–Benson–Bassham cycle by a synthetic malyl-CoA-glycerate carbon fixation pathway. *Nat. Commun.* **2018**, *9*, 2008. [CrossRef] [PubMed]
45. Luo, S.; Lin, P.P.; Nieh, L.-Y.; Liao, G.-B.; Tang, P.-W.; Chen, C.; Liao, J.C. A cell-free self-replenishing CO_2-fixing system. *Nat. Catal.* **2022**, *5*, 154–162. [CrossRef]
46. Luo, S.; Diehl, C.; He, H.; Bae, Y.J.; Klose, M.; Claus, P.; Socorro Cortina, N.; Alvarez Fernandez, C.; Schulz-Mirbach, H.; McLean, R.; et al. Construction and modular implementation of the THETA cycle for synthetic CO_2 fixation. *Nat. Catal.* **2023**, *6*, 1228–1240. [CrossRef]
47. Löwe, H.; Kremling, A. In-depth computational analysis of natural and artificial carbon fixation pathways. *Bio-Des. Res.* **2021**, *2021*, 9898316.

48. Xiao, L.; Liu, G.; Gong, F.; Zhu, H.; Zhang, Y.; Cai, Z.; Li, Y. A minimized synthetic carbon fixation cycle. *ACS Catal.* **2022**, *12*, 799–808. [CrossRef]
49. Ragsdale, S.W. Pyruvate ferredoxin oxidoreductase and its radical intermediate. *Chem. Rev.* **2003**, *103*, 2333–2346. [CrossRef]